

**Design, synthesis, antitrypanosomal activity, DNA/RNA binding and *in vitro*
ADME profiling of novel imidazoline-substituted 2-arylbenzimidazoles**

Andrea Bistrović Popov^a, Luka Krstulović^b, Sanja Koštrun^{c*}, Dubravko Jelić^c, Ana Bokulić^c, Marijana Radić-Stojković^d, Iva Zvonjić^d, Martin C. Taylor^e, John M. Kelly^e, Miroslav Bajić^b, Silvana Raić-Malić^{a*}

^a*Department of Organic Chemistry, Faculty of Chemical Engineering and Technology,
University of Zagreb, Marulićev trg 20, HR-10000 Zagreb, Croatia*

^b*Department of Chemistry and Biochemistry, Faculty of Veterinary Medicine,
University of Zagreb, Heinzelova 55, HR-10000 Zagreb, Croatia*

^c*Fidelta Ltd., Prilaz baruna Filipovića 29, HR-10000 Zagreb, Croatia*

^d*Division of Organic Chemistry and Biochemistry, Laboratory for Biomolecular
Interactions and Spectroscopy, Ruđer Bošković Institute, Bijenička 54,
HR-10000 Zagreb, Croatia*

^e*Department of Infection Biology, London School of Hygiene and Tropical
Medicine, Keppel Street, London, WC1E 7HT, UK*

*Corresponding authors:

Silvana Raić-Malić, e-mail: sraic@fkit.hr; Sanja Koštrun, e-mail: Sanja.Kostrun@fidelta.eu

Abstract

Novel imidazoline benzimidazole derivatives containing diverse substituted phenoxy moieties were synthesized with the aim of evaluating their antitrypanosomal activity, DNA/RNA binding affinity and *in vitro* ADME properties. The presence of the diethylaminoethyl subunit in **18a–18c** led to enhanced antitrypanosomal potency, particularly for **18a** and **18c**, which contain unsubstituted and methoxy-substituted phenoxy moieties. They were found to be > 6-fold more potent against African trypanosomes than nifurtimox. Fluorescence and CD spectroscopy, thermal denaturation assays and computational analysis indicated a preference of **18a–18c** toward AT-rich DNA and their minor groove binding mode. Replacement of the amidine group with less basic and ionisable nitrogen containing moieties failed to improve membrane permeability of the investigated compounds. Due to structural diversification, the compounds displayed a range of physico-chemical features resulting in variable *in vitro* ADME properties, leaving space for further optimization of the biological profiles.

Keywords: Imidazoline-substituted benzimidazole, ADME, DNA binding, *Trypanosoma brucei*

1. Introduction

Trypanosomatid protozoan parasites have a significant socioeconomic impact worldwide [1]. Amongst them are parasites of the *Trypanosoma brucei* species complex, which cause human African trypanosomiasis (HAT), also known as sleeping sickness. In the early stage of the disease, parasites invade the blood and lymphatic system, while in the second stage, they penetrate the blood–brain-barrier (BBB) and enter the central nervous system (CNS), leading to coma and death if untreated [2]. The current drugs used to treat HAT, pentamidine, suramin, melarsoprol and nifurtimox-eflornithine combination therapy (NECT) [1], are toxic and not always effective. Drug-resistance, often related to transporters responsible for the drug uptake, has been widely characterised [5,6]. A further limitation of diamidines, which have high therapeutic interest as antiparasitic agents [7], is the requirement for parenteral administration due to poor oral bioavailability resulting from the high pKa of the amidine functional group [8]. Although the active transport of amidines ensures that they reach the site of action, their permanent charge limits membrane permeability and, thus, oral bioavailability.ref However, the permeability and activity of amidines was successfully modulated by lowering the pKa of bisimidazoline compounds with incorporated halogen or nitrogen atoms [8,9]. To improve chemotherapeutic treatment of HAT, the boron-containing small molecule, acoziborole, was developed as an orally active drug candidate that is efficacious in both stages of the disease [10,11].

Various biological targets have been suggested to account for the antiparasitic activity of trypanocidal drugs, including both mitochondrial and nuclear DNA, heat shock protein 70 (Hsp70) [12], microtubules [13], acidocalcisomes [14], trypanosomatid proteasomes [15] and a range of enzymes [16]. Compounds that act as mitochondrial kinetoplast DNA (kDNA) binders have been shown to selectively target AT-rich DNA and to form a complex in the minor groove of the double helix [17–19].

Previous studies by our group [20–22] and others [23–30] have shown that nitrogen heterocycles, such as benzimidazole derivatives, have good antiprotozoal potency. The 5-nitroimidazole derivative, fexinidazole, has been recently developed as an oral treatment of HAT [31–33] and will be a major advance over the current therapy [34]. In addition, triazolo-containing compounds have demonstrated *in vivo* efficacy for trypanosomiasis that is superior to the clinical drug melarsoprol [35,36]. We have designed imidazoline benzimidazole derivatives with substituted phenoxy moieties to modulate physico-chemical and biological properties (Figure 1). Antitrypanosomal potencies and DNA/RNA binding properties of the

compounds were evaluated. Calculated physico-chemical properties were compared with measured *in vitro* ADME properties, microsomal metabolic stability and membrane permeability.

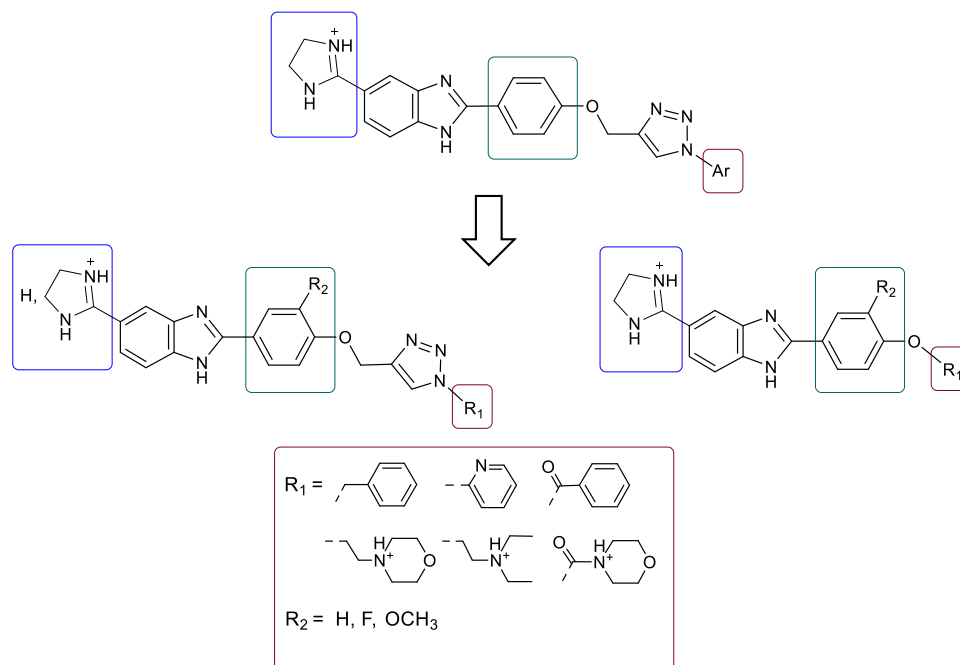
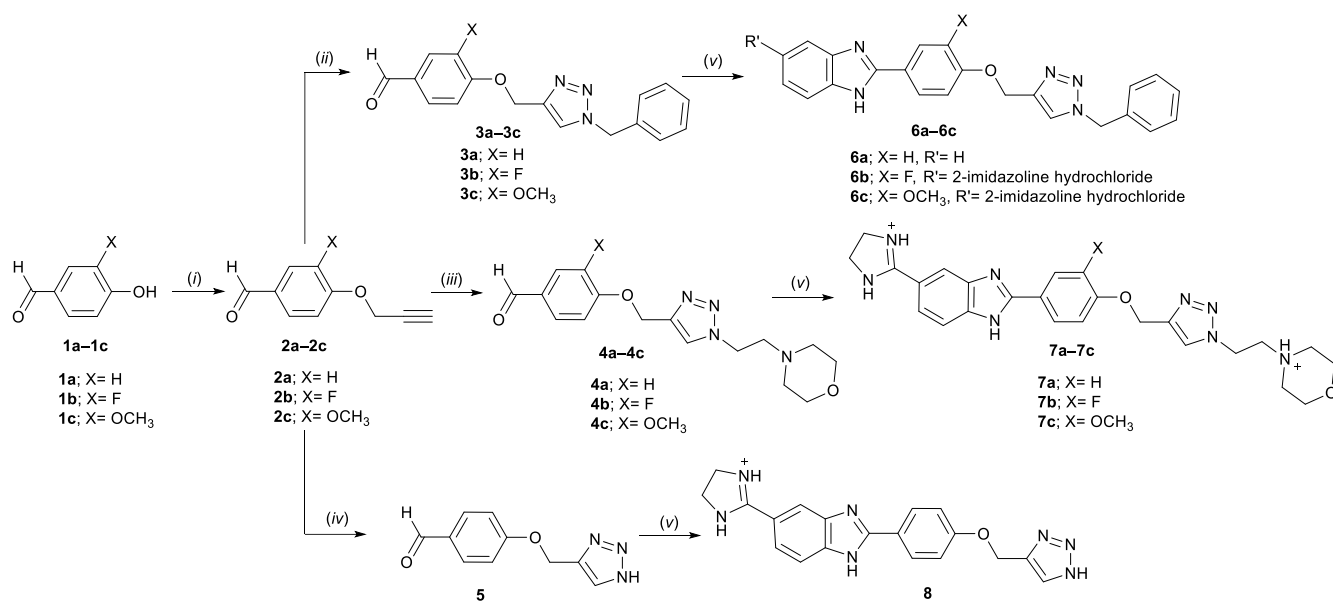


Figure 1. Design of novel imidazoline-substituted benzimidazoles **6a–6c**, **7a–7c**, **8**, **14a–18a**, **14b–18b** and **14c–18c** with a range of cyclic, aromatic as well as ionisable aromatic and aliphatic subunits.

2. Results and discussion

2.1. Chemistry

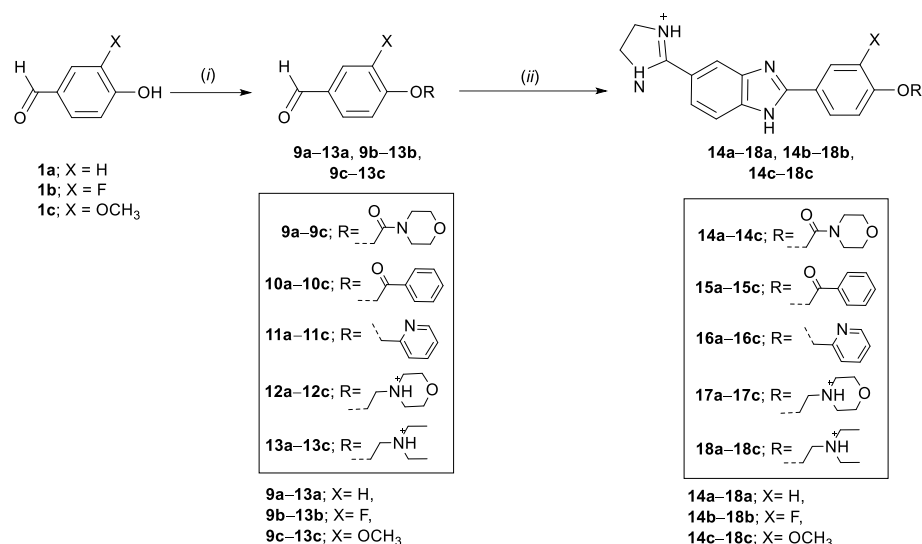
The synthesis of novel 2-aryl substituted benzimidazole derivatives **6a–6c**, **7a–7c**, **8**, **14a–18a**, **14b–18b** and **14c–18c** was carried out as shown in Scheme 1 and 2. Key intermediates for the synthesis of 1,2,3-triazolyl linked 2-aryl benzimidazole derivatives (**6a–6c**, **7a–7c** and **8**) were prepared by regioselective copper(I) catalysed cycloaddition from *O*-propargylated benzaldehydes (**2a–2c**), used as dipolarophiles, and corresponding azides (Scheme 1).



Scheme 1. Reagents and conditions: (i) propargyl bromide, AcCN, K₂CO₃, reflux 8 h; (ii) benzyl chloride, NaN₃, Et₃N, 30 min, rt, Cu(OAc)₂, *t*-BuOH : H₂O = 1 : 1, 24 h; (iii) Cu(OAc)₂, MeOH, reflux, 24 h; (iv) CuI, TMSN₃, DMF : H₂O = 9 : 1, reflux, 6 h; (v) 4-(imidazolin-2-yl)benzene-1,2-diamine/1,2-phenyldiamine, NaHSO₃/*p*-benzoquinone, EtOH, reflux, 8 h.

1-Benzyl-1,2,3-triazole benzaldehydes **3a–3c** were synthesized in excellent yield (82–92%) in a *one-pot click* reaction, 1,3-dipole was formed *in situ* using Cu(II) acetate as a catalyst. 1,3-Dipolar cycloaddition of terminal alkynes (**2a–2c**) and 2-(4-morpholine)ethyl azide yielded the corresponding 1-ethylmorpholine-1,2,3-triazole benzaldehyde precursors **4a–4c**. The ethylmorpholine substituent was introduced to the N-1 position of the 1,2,3-triazole ring to increase solubility of imidazoline-substituted benzimidazole derivatives **7a–7c**. To determine the influence of substituents on the triazole ring on pharmacokinetic properties and trypanosomal activity, non-substituted triazole **5** was prepared with copper(I) iodide and trimethylsilylazide (TMSN₃). Condensation of 4-(1,2,3-triazol-1-yl)benzaldehyde derivatives **3b**, **3c**, **4a–4c** and **5** with 4-(imidazolin-2-yl)benzene-1,2-diamine and NaHSO₃ or *p*-benzoquinone, as an oxidative reagent, afforded the target imidazoline-substituted benzimidazoles (**6b–6c**, **7a–7c** and **8**). The 4-(imidazolin-2-yl)benzene-1,2-diamine was prepared by the Pinner reaction previously reported in literature [37]. Furthermore, to look into the influence of the imidazoline substituent, unsubstituted benzimidazole derivative **6a** was prepared by cyclization of *o*-phenylene diamine with benzaldehyde **3a** in 94% yield. With the aim of assessing the influence of the triazole moiety on the antitrypanosomal activity and pharmacokinetic properties, morpholinoyl (**14a–14c**), benzoyl (**15a–15c**), pyridine (**16a–16c**), ethylmorpholine (**17a–17c**) and diethylaminoethyl (**18a–18c**) substituents were introduced to

the phoxymethylene linker of the imidazoline-substituted benzimidazoles as displayed in Scheme 2. *O*-alkylation of the hydroxybenzaldehydes **1a–1c** with the corresponding halides and K₂CO₃ afforded the benzaldehyde precursors **9a–13a**, **9b–13b** and **9c–13c**, which were converted to targeted 2-aryl-5-(2-imidazoliny)-substituted benzimidazole (**14a–18a**, **14b–18b** and **14c–18c**) hybrids with NaHSO₃ or *p*-benzoquinone.

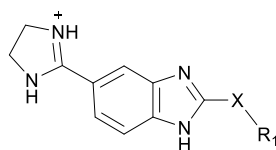


Scheme 2. Reagents and conditions: (i) RCl/RBr, AcCN, K₂CO₃, reflux, 8 h; (ii) 4-(imidazolin-2-yl)benzene-1,2-diamine, NaHSO₃/*p*-benzoquinone, EtOH, reflux, 8 h.

2.2. Antitrypanosomal evaluations

Preliminary screening of 2-aryl-substituted benzimidazole derivatives **6a–6c**, **7a–7c**, **8**, **14a–18a**, **14b–18b** and **14c–18c** against *T. brucei* was performed at different concentrations (100, 10, 1 and 0.1 μg/mL) (Table 1). All compounds displayed 100% growth inhibition at the highest concentration of 100 μg/mL, while at 10 μg/mL, the aromatic phoxymethylene pyridine **16b** had the lowest inhibition (40%). Best selectivity was observed with **6a**, **7a**, **8** and **18a–18c**, which inhibited growth by more than 90% at 1 μg/mL. Thus, from the series of 2-arylbenzimidazoles connected to aromatic and cyclic subunits *via* a 1,2,3-triazole linker, benzimidazole **6a**, which contains benzyl at position N-1 of the triazole and imidazoline-substituted benzimidazoles, **7a** and **7b** with an ethylmorpholine moiety at N-1 of triazole, and **8**, with an unsubstituted triazole ring, showed growth inhibition above 90%. Among the imidazoline benzimidazoles with aromatic and ionisable aliphatic and aromatic subunits directly connected to phoxymethylene, compounds **18a–18c**, with a diethylaminoethyl moiety, exhibited growth inhibition above 90%. At 0.1 μg/mL, only compounds **18a** and **18c** showed any level of inhibition (20%).

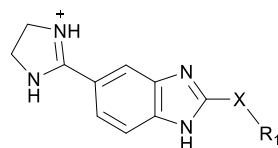
Table 1. Inhibitory properties of compounds **6a–6c**, **7a–7c**, **8**, **14a–18a**, **14b–18b** and **14c–18c** against cultured bloodstream form *Trypanosoma brucei* (Materials and methods).



Cmpd	X	R ₁	% inhibition 100 µg/mL	% inhibition 10 µg/mL	% inhibition 1 µg/mL	% inhibition 0.1 µg/mL
6a	-PhOCH ₂ -		100	100	90	0
6b	-FPhOCH ₂ -		100	90	0	0
6c	-OCH ₃ PhOCH ₂ -		100	100	0	0
7a	-PhOCH ₂ -		100	100	90	0
7b	-FPhOCH ₂ -		100	100	90	0
7c	-OCH ₃ PhOCH ₂ -		100	100	30	0
8	-PhOCH ₂ -		100	100	90	0
14a	-PhOCH ₂ -		100	100	0	0
14b	-FPhOCH ₂ -		100	100	0	0
14c	-OCH ₃ PhOCH ₂ -		100	80	0	0
15a	-PhOCH ₂ -		100	100	0	0
15b	-FPhOCH ₂ -		100	90	0	0
15c	-OCH ₃ PhOCH ₂ -		100	100	0	0
16a	-PhOCH ₂ -		100	100	0	0
16b	-FPhOCH ₂ -		100	40	0	0
16c	-OCH ₃ PhOCH ₂ -		100	100	0	0
17a	-PhOCH ₂ -		100	100	0	0
17b	-FPhOCH ₂ -		100	80	0	0
17c	-OCH ₃ PhOCH ₂ -		100	90	0	0
18a	-PhOCH ₂ -		100	100	100	20
18b	-FPhOCH ₂ -		100	100	90	0
18c	-OCH ₃ PhOCH ₂ -		100	100	100	20

Based on these results, further antitypanosomal activity evaluations were performed for selected compounds **6a**, **7a**, **7b**, **8**, and **18a–18c**, and expressed as the concentration that inhibited growth by 50% (IC₅₀) and 90% (IC₉₀) (Table 2).

Table 2. Antitrypanosomal activity^a of compounds **6a**, **7a**, **7b**, **8**, and **18a–18c** against cultured bloodstream form *Trypanosoma brucei* (Materials and methods).



Cmpd	X	R ₁	<i>T. brucei</i>		L6 cells	S.I. ^c
			IC ₅₀ (μM)	IC ₉₀ (μM)	IC ₅₀ (μM)	IC ₅₀ (Tb/L6)
6a	-PhOCH ₂ -		3.75 ± 0.06	-	17.2 ± 0.8	4.6
7a	-PhOCH ₂ -		>4	-	-	-
7b	-FPhOCH ₂ -		>4	-	-	-
8	-PhOCH ₂ -		>4	-	-	-
18a	-PhOCH ₂ -		0.47 ± 0.02	1.82 ± 0.15	>250	>530
18b	-FPhOCH ₂ -		3.67 ± 0.30	-	>250	>68
18c	-CH ₃ OPhOCH ₂ -		0.71 ± 0.22	1.47 ± 0.22	>250	>350
Nifurtimox^b	-	-	4.4 ± 0.7 ^b	-	-	-

^a *In vitro* activity against bloodstream form *T. brucei* expressed as the concentration that inhibited growth by 50% (IC₅₀) and 90% (IC₉₀). Data are the mean of triplicate experiments ± SEM. ^b Taken from ref. [38].

^c Selectivity index.

Cytotoxicity was assessed using the rat myoblast cell line L6. In terms of trypanosome growth inhibition, imidazoline benzimidazoles **7a**, **7b** and **8**, with the phenoxyethylene-1,2,3-triazole unit, exhibited the lowest activity of the compounds re-tested. Previously, comparing **7a** and **7b** to the corresponding analogues **17a** and **17b**, in which the ethylmorpholine is directly attached to phenoxy core, we had demonstrated that the 1,2,3-triazole linker does improve activity (Table 1). The 2-arylbenzimidazole **8**, which lacks the cationic imidazolino moiety, showed activity (IC₅₀ = 3.75 μM) comparable to that of nifurtimox. However, this compound was also relatively cytotoxic (IC₅₀ = 17.2 μM) with a selectivity index (S.I.) of 4.6. Introduction of the diethylaminoethyl substituent attached to phenoxyethylene in **18a–18c** led to considerably increased and selective activity, particularly **18a** and **18c** that exhibited IC₅₀ values in sub-micromolar range (**18a**: IC₅₀ = 0.47 μM, IC₉₀ = 1.82 μM; **18c**: IC₅₀ = 0.73 μM, IC₉₀ = 1.47 μM). These compounds were non-cytotoxic (S.I. > 530). Interestingly, addition of the electron-withdrawing fluorine into **18b** resulted in a 6-fold reduction in antitrypanosomal activity compared to non-substituted structural congener **18a**, whereas analogue **18c**, with an electron-donating methoxy group showed comparable activity to **18a**.

2.3. DNA and RNA binding study

Based upon antitrypanosomal activity, compounds **18a–18c** were selected for the binding study with DNA and RNA. As previously mentioned, dicationic molecules with antitrypanosomal activity, such as the bis(2-aminoimidazoline) drugs, were found to be DNA minor groove binders, with selectivity toward AT-sequences [18,39]. According to literature data, this selectivity is predominantly responsible for their antitrypanosomal activity [18,40]. Thus, the aim of this study was to further examine DNA and RNA interactions with highly active trypanocides **18a–18c**. Evaluated compounds were dissolved in redistilled water. Those solutions were used for measurements in aqueous buffer (pH = 7, sodium cacodylate buffer, $I = 0.05 \text{ mol dm}^{-3}$). The UV/Vis spectra (Figures S1-S5, Supporting Information, SI) of buffered solutions of **18a–18c** were proportional to their concentrations up to $c = 2 \times 10^{-5} \text{ mol dm}^{-3}$, suggesting that these compounds do not aggregate by intermolecular stacking at the experimental conditions used. The absorption maxima and the corresponding molar extinction coefficients (ϵ) are given in Table S1 (SI). Changes in the UV/Vis spectra of the compounds as the temperature increased to 95 °C were negligible, and the reproducibility of UV/Vis spectra upon cooling back to 25 °C was excellent. The excitation spectra agreed well with the corresponding absorption spectra in the region where emission and excitation spectrum do not overlap (Figures S6-S13, SI). Binding of the compounds to DNA and RNA polynucleotides was monitored with the fluorescence spectroscopy. CD titrations and ΔT_m experiments were used to determine the binding modes (intercalation, groove binding or external binding).

For initial measurements with ds-polynucleotides, we chose *calf thymus* DNA (ctDNA), which represents a classical B-helix, and poly A – poly U as a model for RNA, with a characteristic A-helical structure of a wide and shallow minor groove and a deep and narrow major groove [41]. After acquiring preliminary results with ctDNA, we decided to perform experiments with synthetic polynucleotides, poly(dAdT)₂ and poly(dGdC)₂, both of which form a classical B-helix, but in the case of the latter, with a minor groove that is sterically hindered by the amino groups of guanine [42]. Polynucleotide addition to compound solutions resulted in an emission increase of **18c**, and fluorescence quenching of **18a** and **18b** (Figure 2, Table 3).

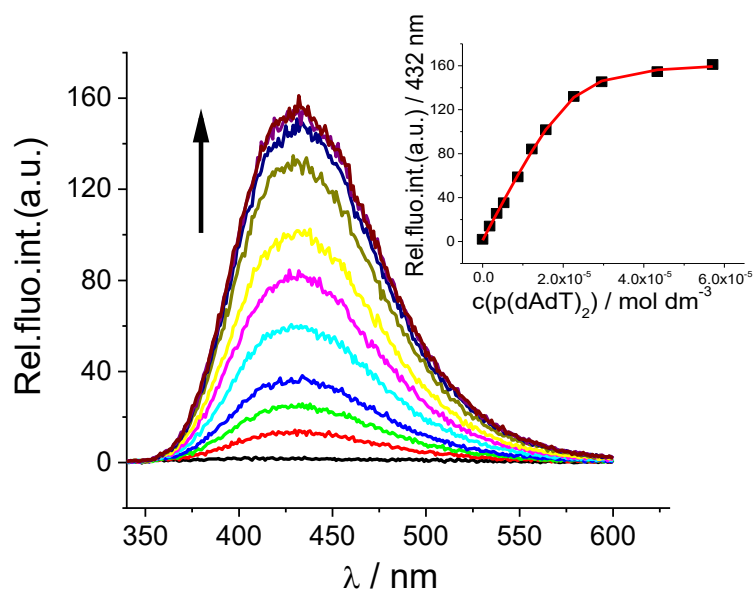


Figure 2. Changes in fluorescence spectrum of **18c** ($c = 1 \times 10^{-6} \text{ mol dm}^{-3}$, $\lambda_{\text{exc}} = 320 \text{ nm}$) upon titration with poly(dAdT)₂ ($c = 1.7 \times 10^{-6} - 5.7 \times 10^{-5} \text{ mol dm}^{-3}$); Inset: dependence of **18c** absorbance at $\lambda = 432 \text{ nm}$ on $c(\text{poly}(\text{dAdT})_2)$, at pH = 7, sodium cacodylate buffer, $I = 0.05 \text{ mol dm}^{-3}$.

18a and **18b** showed dual fluorimetric responses in titrations with AT-DNA (poly(dAdT)₂). First additions of this polynucleotide induced a decrease in **18a** and **18b** fluorescence, while further aliquots yielded a significant fluorescence increase. Unlike **18a** and **18b**, the emission maximum of **18c** did not shift on its binding to most of studied polynucleotides. Fluorescence changes of **18c** with GC-DNA were too small for accurate calculation of binding constants (Table 3).

Table 3. Binding constants ($\log K_s$)^a and ratios n^b ([bound compound]/[polynucleotide phosphate]) calculated from the fluorescence titrations of **18a–18c** with ds-polynucleotides at pH = 7.0 (buffer sodium cacodylate, $I = 0.05 \text{ mol dm}^{-3}$).

	ctDNA			poly A - poly U			p(dAdT) ₂			p(dGdC) ₂		
	$\log K_s$	n	I/I_0^d	$\log K_s$	n	I/I_0^d	$\log K_s$	n	I/I_0^d	$\log K_s$	n	I/I_0^d
18a	5.9	0.2	0.5	5.1	0.2	0.4	5.2	0.1 ^c	2.0	5.3	< 0.1	< 0.1
18b	6.0	0.1	0.3	4.9	0.2	0.2	6.4	0.1 ^c	1.3	4.5	0.4	< 0.1
18c	6.8	< 0.1	43.4	5.4	< 0.1	23.7	7.1	< 0.1	146	- ^e	- ^e	- ^e

^a Accuracy of $n \pm 10 - 30\%$, consequently $\log K_s$ values vary in the same order of magnitude;

^b Processing of titration data by means of Scatchard equation [43] gave values of ratio n [bound compound]/[polynucleotide]; correlation coefficients were >0.99 for most of calculated K_a ;

^c In case of **18a** and **18c** with poly(dAdT)₂, $\log K_a$ values (part of titration experiment where emission increased) were re-calculated for fixed $n = 0.1$ due to a more reliable fit than with free stoichiometry; $\log K_a$ values could not be calculated from part of titration where **18a** and **18c** emission decreased since these changes were too small for accurate calculation of binding constants;

^d I_0 – starting fluorescence intensity of **18a–18c**; I – fluorescence intensity of **18a–18c**/polynucleotide complex calculated by Scatchard equation;

^e Fluorescence changes of studied compound with polynucleotides were too small for accurate calculation of binding constants.

Interestingly, **18a–18c**, that differ only in the phenyl substitution (H vs F vs OCH₃), caused opposite fluorimetric changes on interaction with the studied polynucleotides. While addition of **18a** and **18b** caused a decrease in fluorescence in the presence of DNA/RNA, the addition of any polynucleotides resulted exclusively in a strong emission increase of **18c**, which may be ascribed to an increased electron density in the phenyl ring due to the electron-donating methoxy group (Figures S14-S25, SI).

The binding constants K_s and ratios n [bound compound]/[DNA/RNA] obtained by processing of fluorimetric titration data with the Scatchard equation [43] are summarized in Table 3. All compounds showed greater affinity toward DNA, especially AT-DNA. In particular, **18c** exhibited AT-DNA selectivity over GC-DNA.

Non-covalent binding of small molecules to ds-polynucleotides usually has certain effects on the thermal stability of helices, thus, giving different melting temperature (T_m) values. Melting temperature depends on both the length and the specific nucleotide sequence composition of the polynucleotide. It can be also influenced by salt concentration and pH. Differences between the T_m value of the free polynucleotide and that obtained in complex with small molecules (ΔT_m value) is an important factor in the characterisation of small molecule-ds-polynucleotide interactions [44]. All studied compounds showed a smaller stabilization effect of ds-RNA (poly A - poly U) compared to ds-DNA (Table 4).

Table 4. The ΔT_m^a values (°C) of ds-polynucleotides upon addition of ratio $r^b = 0.3$ and $r^b = 0.5$ of **18a–18c** at pH = 7.0 (sodium cacodylate buffer, $I = 0.05 \text{ mol dm}^{-3}$).

	ctDNA	poly A – poly U	poly (dA – dT) ₂
18a	6.4	4.5	17.9
18b	4.5	2.4	14.7
18c	7.2	2.3	19.3

^a Error in ΔT_m : ± 0.5 °C;

^b $r = [\text{compound}]/[\text{polynucleotide}]$

Furthermore, all compounds showed a significant but smaller stabilization effect toward mixed DNA basepairs than to AT-DNA. This difference in stabilization effect can be explained by ctDNA composition which contains 58% AT and 42% GC nucleobases (Figure 3) [45].

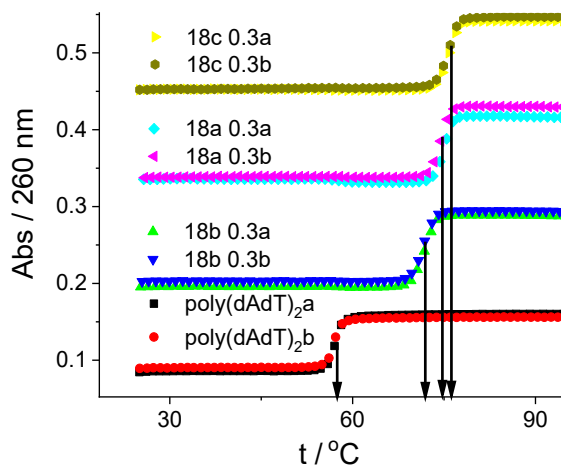


Figure 3. Melting curve of poly(dAdT)₂ upon addition of ratio, r ([compound]/ [polynucleotide]) = 0.3 of **18a–18c** at pH = 7.0 (buffer sodium cacodylate, $I = 0.05 \text{ mol dm}^{-3}$).

Compounds **18a**, without a substituent on the phenyl, and **18c**, with a methoxy-substituted phenyl moiety, showed the best stabilization effect of AT-DNA (Figure 3). Such AT preference is characteristic of small molecules that bind into a minor groove of ds-polynucleotides [19,45]. In the case of ds-RNA, the minor groove is not the probable binding site with these compounds, since it is broad and shallow, in contrast to the deep and narrow minor groove of the ds-DNA [42].

To get insight into conformational changes in the secondary structure of polynucleotides upon small molecule binding, CD spectroscopy was employed [46]. Additional information on the ligand-polynucleotide complexes can be acquired *via* an induced CD (ICD) signal of achiral small molecules when they form complexes with ds-polynucleotides. From this, a mutual orientation of the small molecule and polynucleotide chiral axis can be derived, giving useful information on the modes of interaction [47,48]. The ICD signals observed at $\lambda > 300 \text{ nm}$ can be attributed solely to the studied achiral compounds, since they display UV/Vis spectra in this region while polynucleotides do not (Figures S1-S4, SI).

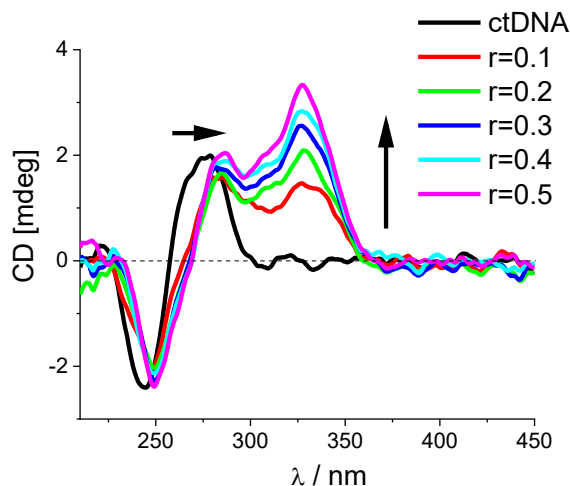


Figure 4. CD titration of poly(dAdT)₂ ($c = 3.0 \times 10^{-5} \text{ mol dm}^{-3}$) with **18a** at molar ratios $r = [\text{compound}]/[\text{polynucleotide}]$ (pH = 7.0, buffer sodium cacodylate, $I = 0.05 \text{ mol dm}^{-3}$).

Addition of the compounds resulted in a decreased CD spectra of RNA and DNA polynucleotides (Figures S29-S30, SI). Conversely, an increase of CD spectra of poly(dGdC)₂ was noticed on addition of all the studied compounds. All compounds exhibited positive induced CD spectra (ICD) with ctDNA and poly(dAdT)₂ in the region from 330-340 nm (Figures S29 and S30, SI). Such changes were observed for cationic benzimidazoles and indoles that were found to be minor groove binders [19,48]. The positive ICD spectra, located around 336 nm, were also observed in titrations of poly A – poly U with all compounds studied (Figure S29, SI). Additionally, clear isodichroic points were observed in titrations of **18a** with AT-DNA and **18c** with poly A – poly U, suggesting one dominant interaction mode of these compounds with the DNA/RNA chiral axis [47,48].

A positive ICD band, with an intensity similar or stronger than the CD band of DNA/RNA, strongly supports the minor groove binding to DNA, or the major groove binding to ds-RNA [49]. Thus, it can be concluded that the compounds bind to minor groove of ds-DNA and to major groove of ds-RNA. This is additionally supported by thermal stabilization of ds-polynucleotides (Table 4) and the binding constants $\geq 10 \mu\text{M}$ (Table 3). Appearance of a dual fluorimetric response in the titrations of **18a** and **18b** with AT-DNA, suggests two different modes of binding, probably monomer binding inside the groove at ratios $r[\text{18a}, \text{18b}]/[\text{poly(dAdT)}_2] < 0.2$ and formation of lower order aggregates of **18a** and **18b** at ratios $r > 0.2$. The intensity of the CD spectrum of poly(dGdC)₂ significantly increased upon addition of all compounds and there were no ICD bands at wavelengths longer than 300 nm. Such changes

suggest a non-intercalative mode of binding, probably aggregation along the polynucleotide backbone, most likely inside the hydrophobic major grooves [50].

2.4. Computational analysis of imidazoline-substituted benzimidazoles binding to DNA

To further investigate the results obtained by fluorescence and CD spectroscopy, binding of **18a–18c** to the DNA minor groove at the molecular level, as well as their selectivity towards the AT sequences, were investigated by computational methods.

Available X-ray structures of DNA complexes with binders, structurally related to imidazoline-substituted benzimidazoles, were retrieved from the Protein Databank [51–53] and retrieved DNA-ligand complexes and interactions were analysed (pdb codes: 1D30, 1D64, 1DNH, 109D, 1FTD, 1M6F, 1Z8V, 1JTL, 1RMX, 2DND, 2B0K, 2GYX, 442D, 445D, 403D, 458D/459D, 4AH1, 432D, 5T4W, 5LIT, 6BNA, 6EL8). Further computational experiments were carried out using the crystal structure of the DB921-D(CGCGAATTCGCG)₂ complex (pdb: 2B0K) and the structure of the DNA duplex d(AAATTT)₂ with the potential antiparasitic drug 6XV (pdb: 5LIT). These were used as reference structures of AT-rich DNA complexes, in addition to the crystal structure of the Forkhead domain of human FOXN1 in complex with human ctDNA (6EL8) for selectivity investigation. Structures of inhibitors and interactions with DNA are given in Figure 5.

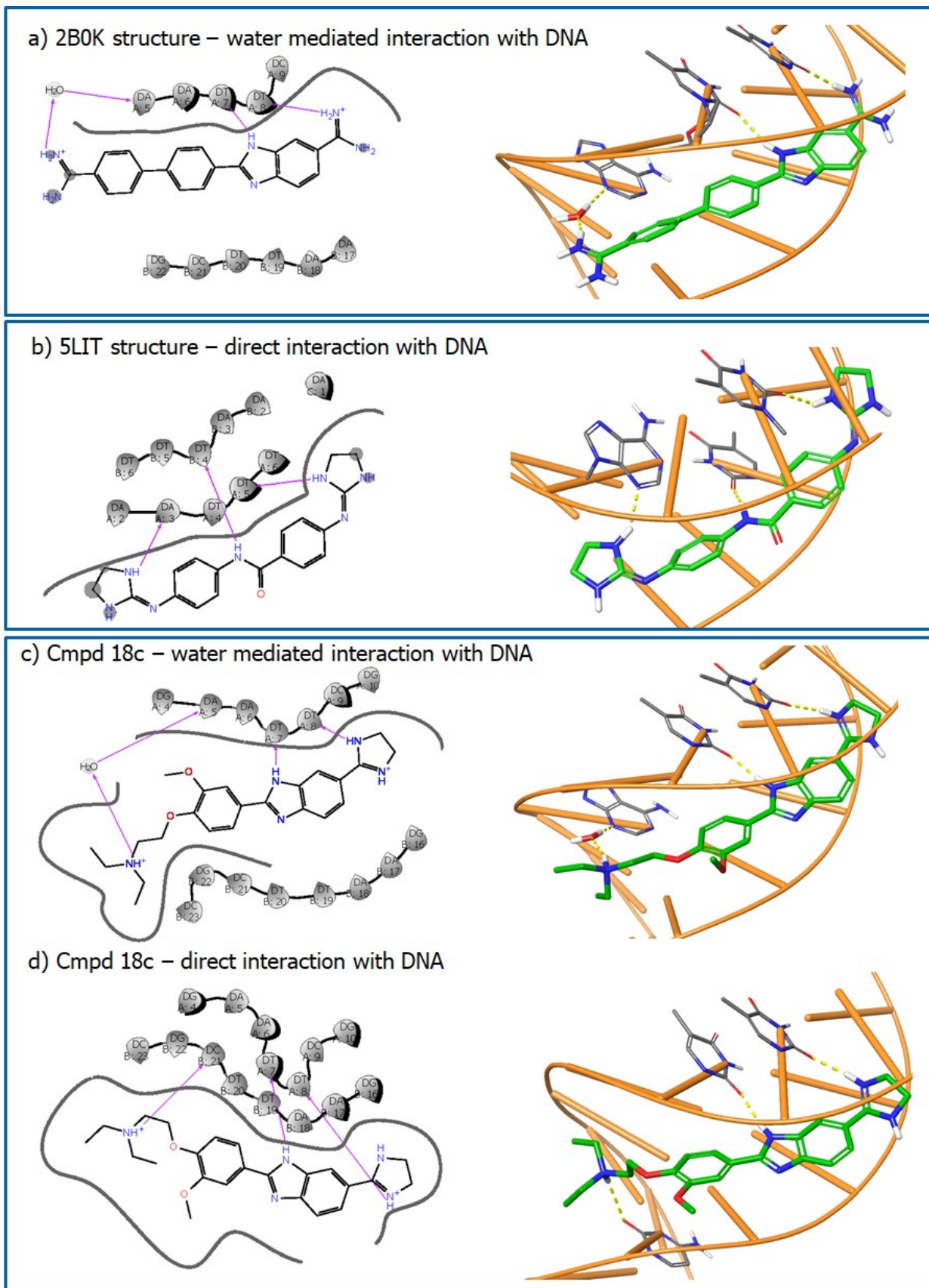


Figure 5. DNA interactions with known ligands (pdb codes: 2B0K and 5LIT) and compound 18c.

Compounds **18a–18c** were docked to the X-ray templates of DNA as described in the Methods section. Both, water mediated and direct binding to the minor groove of the DNA were examined. Complexes were further optimized by the MMGBSA method, and the energy of interactions is shown in Table 5.

Table 5. Ligand $\Delta G(\text{int})/\text{kcalmol}^{-1}$ with AT-rich DNA and ctDNA.

Cmpd	AT-rich DNA	AT-rich DNA + water	ctDNA	ctDNA + water
2B0K ligand	-80	-84	-68	-73
18c	-100	-75	-84	not forming

Compounds **18a–18c** could bind directly as well as through water mediated interactions to compensate the deviations from isohelical structures as shown in Figure 5. Both complexes form three hydrogen-bonds with the DNA bases, with the only difference noticed being for the interaction of the diethylamino group. In the case of water mediated binding, all hydrogen bonds are formed with chain A of the DNA helix, while in the direct complex, the diethylamino group forms a hydrogen bond with the C21 of the chain B. At 2.5 Å, this is slightly longer than the other two strong H-bonds of 1.8 and 2.0 Å, respectively.

For the most active compounds shown in the Table 5, deviation from the ideal isohelical structure is around 20°, comparable to a DAPI molecule (pdb: 1D30), and the deviation from the linear geometry is around 30°.

As already shown for a number of minor groove binders [8,53–55], lack of an isohelical structure could be efficiently compensated for by water mediated interactions. In order to investigate which complex would be energetically favourable, docked geometries were re-optimised and free energies of interaction were calculated by the MMGBSA method. We employed molecular mechanics to estimate the strength of interaction and a generalised Born model and solvent accessibility method to implicitly describe solvent effects. Results are shown in Table 5 for the 2B0K ligand, as reference, and compound **18c**. It can be seen, from the calculated free energies, that the 2B0K ligand forms a more stable water mediated complex, while for compound **18c**, direct interactions are more favourable. This is not surprising since the flexible diethylaminoethylene chain can easily adopt a conformation that enables the formation of H-bonds with DNA bases. In addition, molecular dynamic simulations were performed to check the dynamics of ligand-DNA interactions. In the case of 2B0K, two direct and one water mediated hydrogen bond is formed and maintained throughout the whole

simulation time. For the **18c** ligand, in addition to two direct H-bonds, a third H-bond is formed both directly and bridged by a water molecule, increasing the probability of strong interaction. Findings from these structural studies are in agreement with the observed antitrypanosomal activity, since the most active compounds, **18a–18c**, possess a flexible diethylaminoethyl group. In contrast, compounds with more rigid and 3D shaped morpholine, pyridine and phenyl moieties exhibit lower activity. Furthermore, compound **18c** binds with higher selectivity to AT-rich DNA in comparison to ctDNA, as shown by calculated free binding energies (Table 5).

To further explore the dynamics of water mediated ligand-DNA interactions, molecular dynamic simulations in water as the solvent were performed for 20 ns at room temperatures to ensure stability of the DNA oligomers [56]. Simulations were carried out for 2B0K and **18c** ligands, and the MMGBSA optimised complex structures were used as starting points. The average number of direct H-bonds during the simulation is in agreement with docking and MMGBSA predictions, while water mediated H-bonds are more dynamic and occur with lower frequency than direct H-bonds, as shown in Figure 6.

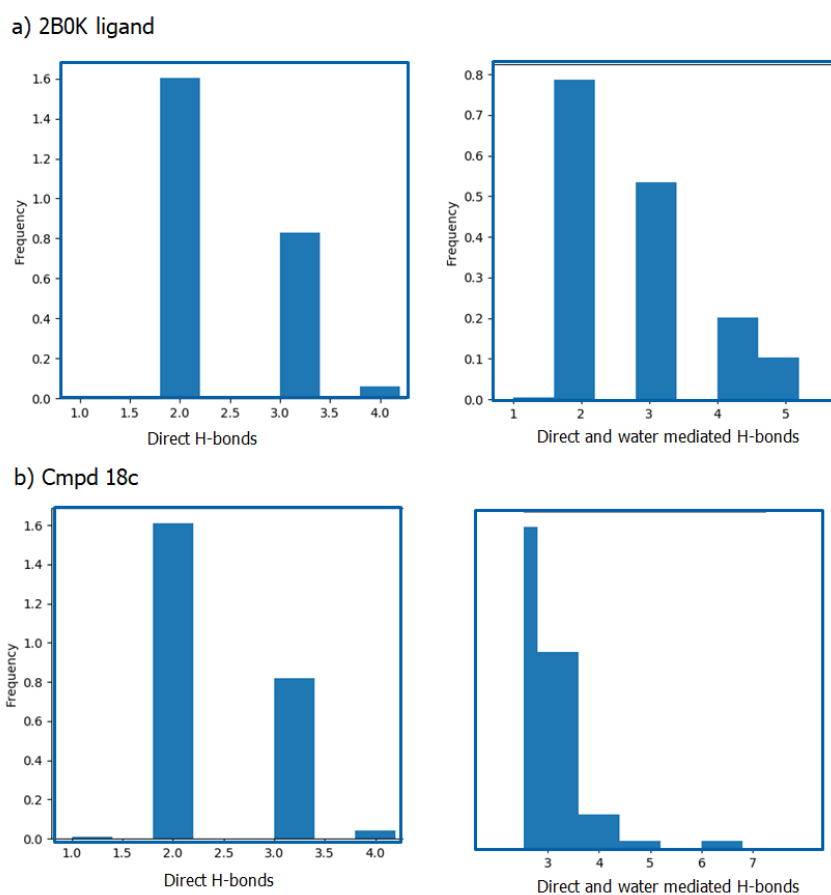


Figure 6. Average number of direct and water mediated H-bonds during MD simulation for a) 2B0K and b) **18c** ligands.

2.5. *In vitro* ADME profiling

Metabolic stability in mouse liver microsomes and permeability in the MDCKII-hMDR1 assay were determined for synthesized imidazoline-substituted benzimidazole derivatives and the results are shown in Table 6. In addition, lipophilicity, solubility, potential for CYP inhibition and metabolism, binding to plasma proteins and structural parameters were calculated by ACD Percepta software (Table 6). Metabolic studies have shown that majority of compounds have low (< 30% LBF) to moderate clearance (30-70% LBF), while compounds **6a–6c** and **15a–15c** with phenyl ring have high clearance (> 70% LBF), indicating the impact of the substituent at the triazole and phenoxy unit on metabolic stability. Thus, in the series of compounds with the triazole moiety, imidazoline benzimidazole **8**, with an unsubstituted triazole showed low clearance and high stability in microsomes, whereas ethylmorpholine-substituted analogues **7a–7c** and, particularly, the benzyl-substituted derivatives **6a–6c**, exhibited reduced microsomal stability. Among the series containing a phenoxy core directly substituted with cyclic, aromatic and aliphatic moieties, morpholinoyl (**14a–14c**), methylpyridine (**16a–16c**) and diethylaminoethyl (**18a–18c**) substitution improved the metabolic stability.

Although compounds were designed to contain one, instead of two amidine moieties, they were all characterized by low membrane permeability ($P_{app}(AB) < 2 \times 10^{-6}$ cm/s). High efflux was also measured for compounds **16a**, **16c** and **18a–18c**. A major bottleneck to the membrane permeability is the permanently charged amidine moiety. Compound **6a**, which does not contain an amidine group, has a high AB permeability of 12.49×10^{-6} cm/s. However, the amidine moiety was shown to be important for the DNA binding and active transport into the parasitic cell, as evidenced by the observed antitrypanosomal activity. Therefore, modulation of amidine basicity will be essential in order to increase membrane permeability and to retain biological activity. pKa values were predicted to range from 11 to 13 for amidine moieties, around 9 for aliphatic amines, and around 7 for morpholine derivatives, which is in agreement with the published data [57–59]. Imidazoline benzimidazoles fall in the good lipophilicity range, with a calculated logP spanning from 1.14 to 3.17, and logD from -1.2 to 1.31. Non-amidino benzimidazole **6a** has logP value of 4.15. Binding to plasma proteins (PBP) is predicted to be lower than 91% for imidazoline benzimidazoles, with ethylmorpholine (**7a–7c** and **17a–17c**) and diethylaminoethyl (**18a–18c**), ensuring an acceptable drug free fraction, while compounds **6a–6c** with N-1 benzyl-substituted triazole showed the highest binding (> 99% PBP).

Table 6. Measured metabolic stability in mouse liver microsomes (Pred *in vivo* hep CL) and apparent permeability (P_{app}) in MDCKII-hMDR1 cell assay from apical-to-basolateral (AB) and basolateral-to-apical (BA) side and calculated physicochemical and structural properties.

Measured properties					Calculated properties									
Cmpd	Pred <i>in vivo</i> hep CL [% LBF]	P_{app} (AB) [$\times 10^{-6}$ cm/s]	P_{app} (BA) [$\times 10^{-6}$ cm/s]	Efflux ratio	TPSA ^a	AR ^b	RB ^c	HBD ^d	HBA ^e	LogP	LogD	Solubility	pKa	PPB ^f (%)
6a	74.22	12.49	N/A	N/A	68.6	5	6	1	6	4.15	4.15	Highly insoluble	5.2	99.62
6b	84.37	<0.1	0.09	N/A	93.0	5	7	2	8	3.07	1.21	Insoluble	12.6	98.92
6c	79.00	<0.1	<0.1	N/A	102.2	5	8	2	9	2.67	0.81	Insoluble	10.9	98.98
7a	47.87	1.09	1.18	1.09	105.5	4	8	2	10	1.2	-0.7	Soluble	10.9/7.4	88.65
7b	73.42	0.49	0.80	1.64	105.5	4	8	2	10	1.32	-0.58	Soluble	12.6/7.4	89.15
7c	64.14	0.48	0.89	1.86	114.7	4	9	2	11	1.17	-0.73	Very soluble	10.9	89.55
8	<30	0.46	0.84	1.81	103.9	4	5	3	8	1.58	-0.26	Slightly soluble	11.0	91.08
14a	<30	1.06	1.53	1.44	91.8	3	5	2	8	1.14	-0.72	Slightly soluble	10.9	92.85
14b	34.32	0.86	0.99	1.16	91.8	3	5	2	8	1.27	-0.59	Insoluble	12.6	93.58
14c	<30	1.76	1.38	0.78	101.1	3	6	2	9	0.98	-0.88	Slightly soluble	10.9	88.31
15a	87.06	<0.1	0.11	N/A	79.4	4	6	2	6	3.09	1.23	Insoluble	10.9	99.2
15b	92.59	<0.1	<0.1	N/A	79.4	4	6	2	6	3.17	1.31	Insoluble	12.6	98.15
15c	90.38	<0.1	N/A	N/A	88.6	4	7	2	7	3.08	1.22	Insoluble	10.9	98.63
16a	<30	0.07	0.51	7.82	75.2	4	5	2	6	2.62	0.76	Insoluble	12.7	97.68
16b	<30	<0.1	0.2	>2.4	75.2	4	5	2	6	2.7	0.84	Insoluble	12.6	96.71
16c	<30	0.12	0.52	4.22	84.4	4	6	2	7	2.24	0.38	Insoluble	12.7	96.81
17a	66.97	0.49	0.69	1.40	74.8	3	6	2	7	1.81	-0.09	Soluble	12.7/7.1	82.86
17b	65.49	0.49	0.84	1.70	74.8	3	6	2	7	1.86	-0.03	Soluble	12.5/7.0	86.93
17c	47.79	0.64	0.67	1.04	84.0	3	7	2	8	1.66	-0.25	Soluble	12.7/7.0	82.8
18a	<30	0.27	0.63	2.38	65.5	3	8	2	6	2.99	-0.71	Soluble	12.5/8.9	90.82
18b	<30	0.17	0.49	2.92	65.5	3	8	2	6	2.87	-0.88	Soluble	12.7	89.63
18c	<30	<0.1	0.50	>5.0	74.8	3	9	2	7	2.57	-1.20	Slightly soluble	12.7/9.0	89.41

^a total polar surface area; ^b number of aromatic rings; ^c number of rotatable bonds; ^d number of hydrogen bond donors; ^e number of hydrogen bond acceptors; ^f plasma protein binding.

Compounds containing ionisable groups (**7a–7c**, **17a–17c** and **18a–18c**) are predicted to have good water solubility. Overall, the physico-chemical and *in vitro* ADME properties could be favourably modulated within the current chemical series, with exception of a consistently low membrane permeability.

3. Conclusions

The imidazoline-substituted benzimidazoles with a range of cyclic, aromatic and ionisable aromatic and aliphatic substituents to a phenoxy central core were synthesized and evaluated for their antitrypanosomal activity. Generally, the type of substituents had profound effects on antiprotozoal activities. While a triazole spacer between the phoxymethylene and the ethylmorpholine (in **7a** and **7b**), and the benzyl moiety (in **6a**), led to improved and rather unselective activity, the diethylaminoethyl directly attached to phenoxy in **18a–18c** significantly increased the potency with IC₅₀ values in the range of 0.47 to 3.67 μM. Furthermore, introduction of an electron-withdrawing fluorine (**18b**) resulted in decreased growth inhibition, while non-substituted and electron-donating methoxy-substituted phenoxy moieties (**18a** and **18c**) showed comparable antitrypanosomal activity.

Fluorescence and CD spectroscopy, as well as the thermal denaturation assay showed large stabilization effects of AT-DNA, high binding affinities and large positive ICD spectra for **18a–18c** that point to their preference toward AT-rich DNA sequences and minor groove binding mode. These results were supported by computational analysis, which showed that compounds **18a–18c** with a conformationally unrestricted diethylaminoethyl chain, in comparison to the rigid analogues with cyclic and aromatic moieties, have stronger interaction to DNA and can bind with higher selectivity to AT-rich DNA, in comparison to ctDNA.

In vitro ADME profiling showed that the imidazoline-substituted benzimidazoles with ionisable ethylmorpholine (**7a–7c** and **17a–17c**) and diethylaminoethyl (**18a–18c**) units have favourable ADME properties. However, the low membrane permeability of amidine benzimidazoles suggests further optimization is required in order to modulate amidine basicity [8,9,60] and, therefore, improve permeability and oral bioactivity potential.

4. Material and methods

4.1. General

All the solvents and chemicals were purchased from Aldrich and Acros. Thin layer chromatography was performed on pre-coated Merck silica gel 60F-254 plates, while glass

column slurry-packed under gravity with silica gel (Fluka, 0.063–0.2 mm) was employed for column chromatography. Melting points of compounds were determined using Kofler micro hot-stage. ^1H and ^{13}C NMR spectra were recorded on a Varian Gemini 300 (300 and 75 MHz) or Varian Gemini 600 (600 and 150 MHz). All data were recorded in dimethyl sulfoxide ($\text{DMSO-}d_6$) at 298 K. Chemical shifts were referenced to the residual solvent signal of DMSO at δ 2.50 ppm for ^1H and δ 39.50 ppm for ^{13}C . Individual resonances were assigned on the basis of their chemical shifts, signal intensities, multiplicity of resonances, H–H coupling constants and with the use of a set of 2D experiments.

4.2. Experimental procedures for the preparation of compounds

4-(Prop-2-ynoxy)benzaldehyde (**2a**) [61], 3-methoxy-4-(prop-2-ynoxy) benzaldehyde (**2c**) [62], 4-(imidazolin-2-yl)benzene-1,2-diamine [37], 4-(2-azidoethyl)morpholine [63] were prepared according to known procedure, while compounds 4-(1,2,3-triazol-4-yl)methoxybenzaldehyde (**3a**) [64], 4-[(1-benzyl-1*H*-1,2,3-triazol-4-yl)methoxy]-3-methoxybenzaldehyde (**3c**) [65], 4-(2-morpholino-2-oxoethoxy)benzaldehyde (**9a**) [66], 3-methoxy-4-(2-morpholino-2-oxoethoxy)benzaldehyde (**9c**) [67], 4-(2-oxo-2-phenylethoxy)benzaldehyde (**10a**) [68], 3-methoxy-4-(2-oxo-2-phenylethoxy)benzaldehyde (**10c**) [69], 4-(pyridin-2-yl-methoxy)benzaldehyde (**11a**) [70], 3-fluoro-4-(pyridin-2-yl-methoxy)benzaldehyde (**11b**) [70], 3-methoxy-4-(pyridin-2-yl-methoxy)benzaldehyde (**11c**) [71], 4-(2-morpholinoethoxy)benzaldehyde (**12a**) [72], 3-fluoro-4-(2-morpholinoethoxy)benzaldehyde (**12b**) [73], 3-methoxy-4-(2-morpholinoethoxy)benzaldehyde (**12c**) [74], 4-(2-(diethylamino)ethoxy)benzaldehyde (**13a**) [75], 4-(2-(diethylamino)ethoxy)-3-methoxybenzaldehyde (**13c**) [76], were synthesized according to modified procedures given in the literature.

Preparation of 3-fluoro-4-(prop-2-yn-1-yloxy)benzaldehyde (2b)

To a solution 3-fluoro-4-hydroxybenzaldehyde (5.0 g, 35.7 mmol) in dry ethanol (8–10 mL) K_2CO_3 (1.2 eq.) was added and the mixture was stirred for 30 min followed by addition of propargyl bromide (1.2 eq.). The reaction mixture was stirred overnight at reflux temperature. The course of the reaction was monitored by TLC. Upon completion of the reaction, the solvent was evaporated under reduced pressure and the crude residue was purified by column chromatography with CH_2Cl_2 . Compound **2b** was obtained as yellow solid (4.5 g, 66%, m.p. = 111–115 °C). ^1H NMR (600 MHz, $\text{DMSO-}d_6$) (δ /ppm): 9.88 (1H, d, J = 2.0 Hz, CHO), 7.80

(1H, dd, $J = 8.4, 0.9$ Hz, Ph), 7.73 (1H, dd, $J = 11.3, 1.9$ Hz, Ph), 7.45 (1H, t, $J = 8.3$ Hz, Ph), 5.04 (2H, d, $J = 2.4$ Hz, CH₂), 3.70 (1H, t, $J = 2.4$ Hz, CCH). ¹³C NMR (75 MHz, DMSO) δ 190.8; 190.8 (d, $J_{CF} = 1.8$ Hz, CHO), 153.4; 150.1 (d, $J_{CF} = 247.6$ Hz, Ph-q), 150.2 (Ph-q), 130.4; 130.3 (d, $J_{CF} = 5.1$ Hz, Ph-q), 128.0; 127.9 (d, $J_{CF} = 3.1$ Hz, Ph), 115.6; 115.4 (d, $J_{CF} = 18.4$ Hz, Ph), 115.2; 115.2 (d, $J_{CF} = 1.3$ Hz, Ph), 79.5 (CCH), 78.0 (CCH), 56.7 (OCH₂).

4.2.1. General procedure for synthesis of *N*-1-benzyl-1,2,3-triazole benzaldehydes **3a–3c**

The reaction mixture benzyl chloride (1.1 eq.), NaN₃ (0.9 eq.) and Et₃N (1.3 eq.) was dissolved in *t*-BuOH : H₂O = 1 : 1 (4 mL) and stirred for 30 min. The corresponding terminal alkyne (**2a–2c**) and Cu(OAc)₂ (0.05 eq) were added. The reaction mixture was stirred overnight at room temperature. The solvent was removed under reduced pressure and purified by column chromatography with CH₂Cl₂.

4-[(1-Benzyl-1*H*-1,2,3-triazol-4-yl)methoxy]-3-fluorobenzaldehyde (**3b**)

According to the general procedure from compound **2b** (250 mg, 1.40 mmol) compound **3b** was prepared as colourless oil (378.7 mg, 87%). ¹H NMR (300 MHz, DMSO-*d*₆) (δ /ppm): 9.87 (1H, d, $J = 2.1$ Hz, 1H), 8.35 (1H, s, H5'), 7.81–7.77 (1H, m, Ph), 7.70 (1H, dd, $J = 11.3, 1.9$ Hz, Ph), 7.60 (1H, t, $J = 8.3$ Hz, Ph), 7.39–7.29 (5H, m, Ph), 5.63 (2H, s, CH₂), 5.37 (2H, s, CH₂). ¹³C NMR (75 MHz, DMSO-*d*₆) (δ /ppm): 191.0; 190.9 (d, $J_{CF} = 1.7$ Hz, CHO), 153.4; 150.1 (d, $J_{CF} = 247.1$ Hz, Ph-q) 151.2; 151.1 (d, $J_{CF} = 10.9$ Hz, Ph-q), 141.9 (C4'), 135.9 (Ph-q), 130.0; 130.0 (d, $J_{CF} = 5.0$ Hz, Ph-q), 128.9 (Ph), 128.3 (Ph), 128.0 (Ph), 125.3 (C5'), 115.5; 115.3 (d, $J_{CF} = 18.3$ Hz, Ph), 115.2; 115.1 (d, $J_{CF} = 1.5$ Hz, Ph), 62.3 (OCH₂), 53.0 (CH₂).

4-[(1-Benzyl-1*H*-1,2,3-triazol-4-yl)methoxy]-3-methoxybenzaldehyde (**3c**)

According to the general procedure from compound **2c** (250 mg, 1.31 mmol) compound **3c** was prepared as colourless oil (345.6 mg; 82 %). ¹H NMR (600 MHz, DMSO-*d*₆) (δ /ppm): 9.85 (1H, s, CHO), 8.31 (1H, s, H5'), 7.55 (1H, dd, $J = 8.3, 1.9$ Hz, Ph), 7.41–7.31 (7H, m, Ph), 5.62 (2H, s, CH₂), 5.26 (2H, s, CH₂), 3.80 (3H, s, OCH₃). ¹³C NMR (151 MHz, DMSO-*d*₆) (δ /ppm): 191.4 (CHO), 152.8 (Ph-q), 149.4 (Ph-q), 142.3 (C4'), 135.9 (Ph-q), 123.0 (Ph-q), 128.8 (Ph), 128.2 (Ph), 128.0 (Ph), 125.7 (Ph), 125.0 (C5'), 112.8 (Ph), 109.9 (Ph), 61.8 (OCH₂), 55.5 (CH₃), 52.9 (CH₂).

4.2.2. General procedure for the synthesis of **4a–4c**

4-(2-Chloroethyl)morpholine 156 (3.0 g; 16.12 mmol) was dissolved in water (16.12 mL) and NaN₃ (3.15 g; 48.37 mmol) was added. The reaction mixture was stirred at 80 °C for 16 h. After completion of the reaction, the mixture was cooled and the pH was adjusted to 10 using KOH. The mixture was extracted with diethyl ether (3 × 50 mL). The organic layer was dried over anhydrous MgS, filtered, and the filtrate was evaporated under reduced pressure at room temperature. The unstable azide (600 mg, 3.84 mmol) was immediately used for the click reaction with the corresponding *O*-propargylated benzaldehyde **2a–2c** (3.84 mmol) and Cu(OAc)₂ (34.9 mg; 0.19 mmol) in methanol (4 mL). The reaction mixture was stirred at reflux temperature overnight. The course of the reaction was monitored by TLC. Upon completion of the reaction, the solvent was evaporated under reduced pressure and the residue was purified by column chromatography on eluent CH₂Cl₂ : CH₃OH = 50 : 1.

4-[(1-(2-Morpholinoethyl)-1*H*-1,2,3-triazol-4-yl)methoxy}benzaldehyde (4a)

According to the general procedure from compound **2a** (615.06 mg, 3.84 mmol) compound **4a** was prepared as colourless crystals (1.01 g, 83%, m.p. = 109–113 °C). ¹H NMR (300 MHz, DMSO-*d*₆) (δ/ppm): 9.88 (1H, s, CHO), 8.26 (1H, s, H5'), 7.88 (2H, d, *J* = 8.8 Hz, Ph), 7.24 (2H, d, *J* = 8.7 Hz, Ph), 5.29 (2H, s, CH₂), 4.50 (2H, t, *J* = 6.3 Hz, CH₂CH₂), 3.55–3.47 (4H, m, CH₂-morpholine), 2.73 (2H, t, *J* = 6.3 Hz, CH₂CH₂), 2.44–2.37 (4H, m, CH₂-morpholine). ¹³C NMR (151 MHz, DMSO-*d*₆) (δ/ppm): 191.3 (CHO), 162.9 (Ph-q), 141.7 (C4'), 131.7 (Ph), 129.9 (Ph-q), 125.1 (C5'), 115.2 (Ph), 66.1 (CH₂-morpholine), 61.5 (OCH₂), 57.2 (CH₂CH₂), 52.9 (CH₂-morpholine), 46.6 (CH₂CH₂).

3-Fluoro-4-[[1-(2-morpholinoethyl)-1*H*-1,2,3-triazol-4-yl)methoxy}benzaldehyde (4b)

According to the general procedure from compound **2b** (684.13 mg, 3.84 mmol) compound **4b** was prepared as yellow crystals (1.03 g, 80%, m.p. = 89–93°C). ¹H NMR (300 MHz, DMSO-*d*₆) (δ/ppm): 9.87 (1H, d, *J* = 2.0 Hz, CHO), 8.29 (1H, s, H5'), 7.79 (1H, d, *J* = 8.5 Hz, Ph), 7.70 (1H, dd, *J* = 11.3, 1.8 Hz, Ph), 7.61 (1H, t, *J* = 8.3 Hz, Ph), 5.38 (2H, s, CH₂), 4.50 (2H, t, *J* = 6.2 Hz, CH₂CH₂), 3.57–3.42 (4H, m, CH₂-morpholine), 2.73 (2H, t, *J* = 6.2 Hz, CH₂CH₂), 2.44–2.32 (4H, m, CH₂-morpholine). ¹³C NMR (75 MHz, DMSO-*d*₆) (δ/ppm): 190.8; 190.8 (d, *J*_{CF} = 1.7 Hz, CHO), 153.3; 150.0 (d, *J*_{CF} = 247.0 Hz, Ph-q), 151.2; 151.0 (d, *J*_{CF} = 10.8 Hz, Ph-q), 141.2 (C4'), 129.9; 129.9 (d, *J*_{CF} = 5.0 Hz, Ph-q), 128.2; 128.1 (d, *J*_{CF} = 3.0 Hz, Ph), 125.5 (C5'), 115.4; 115.2 (d, *J*_{CF} = 18.3 Hz, Ph), 115.1; 115.1 (d, *J*_{CF} = 1.5 Hz, Ph), 66.1 (CH₂-morpholine), 62.3 (OCH₂), 57.3 (CH₂CH₂), 52.9 (CH₂-morpholine), 46.5 (CH₂CH₂).

3-Methoxy-4-[[1-(2-morpholinoethyl)-1*H*-1,2,3-triazol-4-yl]methoxy]benzaldehyde (**4c**)

According to the general procedure from compound **2c** (729.83 mg; 3.84 mmol) compound **4c** was prepared as white solid (1.3 g, 98%, m.p. = 142–146 °C). ¹H NMR (300 MHz, DMSO-*d*₆) (δ/ppm): 9.85 (1H, s, CHO), 8.25 (1H, s, H5'), 7.56 (1H, dd, *J* = 8.2, 1.8 Hz, Ph), 7.45–7.33 (2H, m, Ph), 5.27 (2H, s, CH₂), 4.50 (2H, t, *J* = 6.3 Hz, CH₂CH₂), 3.81 (3H, s, OCH₃), 3.54–3.49 (4H, m, CH₂-morpholine), 2.74 (2H, t, *J* = 6.3 Hz, CH₂CH₂), 2.44–2.37 (4H, m, CH₂-morpholine). ¹³C NMR (75 MHz, DMSO-*d*₆) (δ/ppm): 191.3 (CHO), 152.8 (Ph-q), 149.3 (C4'), 141.7 (Ph-q), 129.9 (Ph-q), 125.7 (Ph), 125.3 (C5'), 112.6 (Ph), 109.7 (Ph), 66.0 (CH₂-morpholine), 61.7 (OCH₂), 57.3 (CH₂CH₂), 55.5 (OCH₃), 52.9 (CH₂-morpholine), 46.5 (CH₂CH₂).

4.2.3. Preparation of 4-[[1*H*-1,2,3-triazol-4-yl]methoxy]benzaldehyde (**5**)

Compound **2a** (400 mg, 2.30 mmol) was dissolved in DMF : MeOH = 9 : 1 (4.60 mL), then TMSN₃ (0.45 mL, 3.44 mmol) and CuI (21.9 mg, 0.12 mmol) were added to the reaction mixture and stirred overnight at 100 °C. After completion the reaction, mixture was evaporated to dryness and the crude residue was purified by column chromatography (CH₂Cl₂ : CH₃OH = 100 : 1). Compound **5** was obtained as white solid (355.8 mg, 76%, m.p. = 120–123 °C). ¹H NMR (300 MHz, DMSO-*d*₆) (δ/ppm): 15.13 (1H, bs, NH), 9.88 (1H, s, CHO), 8.09–7.99 (1H, m, H5'), 7.88 (2H, d, *J* = 8.8 Hz, Ph), 7.24 (2H, d, *J* = 8.7 Hz, Ph), 5.32 (2H, s, CH₂). ¹³C NMR (75 MHz, DMSO-*d*₆) (δ/ppm): 191.4 (CHO), 162.9 (Ph-q), 131.8 (Ph), 129.9 (Ph-q), 128.0 (C5'), 115.3 (Ph), 61.2 (CH₂).

4.2.4. General procedure for the synthesis of benzimidazole derivatives **6a–6c** and **8**

The reaction mixture of 4-triazolylbenzaldehyde derivative (**3a–3c**, **5**) the corresponding *o*-phenylenediamine and 40% NaHSO₃ (aq) was dissolved in EtOH (15 mL) and stirred under reflux for 6–8 h. After completion of the reaction, NaHSO₃ was filtered and the reaction mixture was evaporated to dryness. Water was added (5 mL) and the mixture was stirred overnight and filtered. The crude residue was dissolved in HCl saturated EtOH (8–10 mL) and stirred for 4 h. Addition of ether resulted in precipitation of products **6a–6c** and **8**. Solid was collected by filtration, washed with anhydrous ether, and dried under vacuum.

2-{4-[[1-Benzyl-1*H*-1,2,3-triazol-4-yl]methoxy]phenyl}-1*H*-benzo[*d*]imidazole (**6a**)

Compound **6a** was prepared using the above described method from **3a** and 1,2-phenylenediamine (55.30 mg, 0.51 mmol) to obtain **6a** as yellow solid (182.3 mg, 94%, m.p. > 250 °C). ¹H NMR (600 MHz, DMSO-*d*₆) (δ/ppm): 8.32 (1H, s, H5'), 8.11 (2H, d, *J* = 8.8 Hz, Ph), 7.59–7.55 (2H, m, H4; H7), 7.40–7.36 (2H, m, H5; H6), 7.36–7.31 (3H, m, Ph), 7.24–7.17 (4H, m, Ph), 5.63 (2H, s, OCH₂), 5.24 (2H, s, CH₂). ¹³C NMR (75 MHz, DMSO-*d*₆) (δ/ppm): 159.4 (Ph-q), 142.7 (C4'), 135.9 (C3/C7a), 128.7 (Ph), 128.1 (Ph), 128.0 (Ph), 127.9 (Ph), 124.7 (C5'), 122.6 (C2), 121.9 (C5/C6), 115.1 (C4/C7), 61.2 (OCH₂), 52.8 (CH₂). Anal. calcd. for C₂₃H₁₉N₅O (*M*_r = 381.43): C 72.42, H 5.02, N 18.36; found: C 72.16, H 4.81, N 18.63.

2-{4-[(1-Benzyl-1*H*-1,2,3-triazol-4-yl)methoxy]-3-fluorophenyl}-5-(imidazolin-2-yl)-1*H*-benzo[*d*]imidazole hydrochloride (6b**)**

Compound **6b** was prepared using the above described method from **3b** (150 mg, 0.48 mmol) and 4-(imidazolin-2-yl)benzene-1,2-diamine (110.2 mg, 0.48 mmol) to obtain **6b** as white solid (79.5 mg, 35%, m.p. = 200–203 °C). ¹H NMR (600 MHz, DMSO-*d*₆) (δ/ppm): 10.83 (2H, s, CNH), 8.45 (1H, s, H4), 8.38 (1H, s, H5'), 7.99–7.96 (2H, m, Ph), 7.98 (1H, d, *J* = 8.5 Hz, H7), 7.88 (1H, d, *J* = 8.6 Hz, H6), 7.65 (1H, t, *J* = 8.6 Hz, Ph), 7.40–7.36 (2H, m, Ph), 7.35–7.32 (3H, m, Ph), 5.64 (2H, s, OCH₂), 5.37 (2H, s, CH₂), 4.02 (4H, s, CH₂CH₂). ¹³C NMR (75 MHz, DMSO-*d*₆) (δ/ppm): 165.0 (CNH), 153.1; 149.9 (d, *J*_{CF} = 244.9 Hz, Ph-q), 152.5; 152.5 (d, *J*_{CF} = 2.4 Hz, C2), 148.8; 148.7 (d, *J*_{CF} = 10.3 Hz, Ph-q), 142.0 (C4'), 135.9 (C7a/C3a), 128.8 (Ph), 128.2 (Ph), 128.0 (Ph), 125.2 (Ph), 123.6 (C5'), 116.6 (C5), 115.8 (C4/C7), 115.4, 115.1 (d, *J*_{CF} = 20.9 Hz, Ph), 62.2 (OCH₂), 52.9 (CH₂), 44.3 (CH₂CH₂). Anal. calcd. for C₂₆H₂₂FN₇O × HCl × 0.5H₂O (*M*_r = 512.97): C 60.88, H 4.72, N 19.11; found: C 60.63, H 4.41, N 19.22.

2-{4-[(1-Benzyl-1*H*-1,2,3-triazol-4-yl)methoxy]-3-methoxyphenyl}-5-(imidazolin-2-yl)-1*H*-benzo[*d*]imidazole hydrochloride (6c**)**

Compound **6c** was prepared using the above described method from **3c** (150 mg, 0.46 mmol) and 4-(imidazolin-2-yl)benzene-1,2-diamine (106.1 mg, 0.46 mmol) to obtain **6c** as white solid (179.4 mg, 81%, m.p. = 197–200 °C). ¹H NMR (600 MHz, DMSO-*d*₆) (δ/ppm): 10.88 (2H, s, CNH), 8.46 (1H, s, H4), 8.35 (1H, s, H5'), 8.16 (1H, s, Ph), 8.08 (1H, d, *J* = 8.3 Hz, H6), 8.02 (1H, d, *J* = 8.3 Hz, H7), 7.92 (1H, d, *J* = 8.5 Hz, Ph), 7.45 (1H, d, *J* = 8.6 Hz, Ph), 7.40–7.29 (5H, m, Ph), 5.63 (2H, s, OCH₂), 5.28 (2H, s, CH₂), 4.03 (4H, s, CH₂CH₂), 3.90 (3H, s, OCH₃). ¹³C NMR (75 MHz, DMSO-*d*₆) (δ/ppm): 165.2 (CNH), 153.6 (C2), 151.0 (Ph-q), 149.5 (Ph-q), 142.6 (C4'), 139.6 (C3a/C7a), 136.1 (Ph-q), 129.0 (Ph), 128.5 (Ph), 128.2 (Ph), 125.3 (C6),

124.0 (C5'), 121.5 (Ph), 118.8 (Ph-q), 117.2 (C5), 115.8 (C4), 114.9 (C7), 113.7 (Ph), 111.1 (Ph), 61.9 (OCH₂), 56.1 (OCH₃), 53.1 (CH₂), 44.6 (CH₂CH₂). Anal. calcd. for C₂₇H₂₅N₇O₂ × HCl × H₂O (*M_r* = 534.01): C 60.73, H 5.28, N 18.36; found: C 60.81, H 5.20 N 18.39.

5-(Imidazolin-2-yl)-2-{4-[(1*H*-1,2,3-triazol-4-yl)methoxy]phenyl}-1*H*-benzo[*d*]imidazole hydrochloride (8)

Compound **8** was prepared using the above described method from **5** (150 mg, 0.74 mmol) and 4-(imidazolin-2-yl)benzene-1,2-diamine (168.83 mg, 0.74 mmol) to obtain **8** as white solid (251.5 mg, 94%, m.p. = 229–232 °C). ¹H NMR (300 MHz, DMSO-*d*₆) (δ /ppm): 10.90 (2H, s, CNH), 8.47 (1H, s, H5'), 8.43 (2H, d, *J* = 8.9 Hz, Ph), 8.07–8.01 (2H, m, H4; H6), 7.94 (1H, d, *J* = 8.6 Hz, H7), 7.35 (2H, d, *J* = 8.9 Hz, Ph), 5.35 (2H, s, CH₂), 4.03 (4H, s, CH₂CH₂). ¹³C NMR (151 MHz, DMSO-*d*₆) (δ /ppm): 164.7 (CNH), 161.6 (C2), 152.7 (Ph-q), 130.1 (Ph), 124.4 (C5'), 117.6 (C4), 115.7 (Ph), 115.5 (C7), 114.6 (C6), 61.2 (CH₂), 44.3 (CH₂CH₂). Anal. calcd. for C₁₉H₁₇N₇O × HCl × 1.5H₂O (*M_r* = 422.87): C 53.97, H 5.01, N 23.19; found: C 53.61, H 4.77, N 23.43.

4.2.5. General procedure for the synthesis of benzimidazole derivatives 7a–7c

The reaction mixture of the corresponding 4-triazolylbenzaldehyde derivative (**4a–4c**), 4-(imidazolin-2-yl)benzene-1,2-diamine (1 eq) and *p*-benzoquinone (1 eq) was dissolved in EtOH (15 mL) and stirred under reflux for 6–8 h. Addition of ether resulted in precipitation of products **7a–7c**. Solid was collected by filtration, washed with anhydrous ether, and dried under vacuum.

5-(Imidazolin-2-yl)-2-{4-[(1-(2-morpholinoethyl)-1*H*-1,2,3-triazol-4-yl)methoxy]phenyl}-1*H*-benzo[*d*]imidazole dihydrochloride (7a)

According to the above-mentioned procedure, from compound **3a** (150 mg, 0.47 mmol) compound **7a** was obtained as grey solid (74.5 mg, 33%, m.p. = 207–210 °C). ¹H NMR (300 MHz, DMSO-*d*₆) (δ /ppm): 11.98 (1H, bs, NH), 10.94 (2H, s, CNH), 8.50–8.40 (4H, m, H4; H5'; Ph) 8.04 (1H, dd, *J* = 8.6, 1.4 Hz, H6), 7.90 (1H, d, *J* = 8.6 Hz, H7), 7.33 (2H, d, *J* = 9.0 Hz, Ph), 5.33 (2H, s, OCH₂), 4.98 (2H, t, *J* = 7.0 Hz, CH₂CH₂), 4.02 (4H, s, CH₂CH₂), 3.97–3.80 (4H, m, CH₂-morpholine), 3.69 (2H, t, *J* = 7.0 Hz, CH₂CH₂), 3.50–3.33 (2H, m, CH₂-morpholine), 3.22–3.03 (2H, m, CH₂-morpholine). ¹³C NMR (75 MHz, DMSO-*d*₆) (δ /ppm): 164.9 (CNH), 161.3 (Ph-q), 153.0 (C2), 142.5 (C4'), 139.1 (Ph-q), 136.5 (C7a), 135.4 (C3a), 129.9 (Ph), 125.5 (C5'), 124.0 (C6), 117.1 (C5), 115.7 (C4), 115.6 (Ph), 114.7 (C7), 63.1 (CH₂-morpholine), 61.4 (OCH₂),

54.1 (CH₂CH₂), 51.2 (CH₂-morpholine), 44.3 (CH₂CH₂), 43.6 (CH₂CH₂). Anal. calcd. for C₂₅H₂₈N₈O₂ × 2HCl × 1.75H₂O (*M*_r = 576.99): C 52.04, H 5.85, N 19.42; found: C 52.27, H 5.97, N 19.26.

5-(Imidazolin-2-yl)-2-{4-[(1-(2-morpholinoethyl)-1*H*-1,2,3-triazol-4-yl)methoxy]-3-fluorophenyl}-1*H*-benzo[*d*]imidazole dihydrochloride (7b)

According to the above-mentioned procedure, from compound **3b** (150 mg, 0.45 mmol) compound **7b** was obtained as brown solid (169.6 mg, 72%, m.p. = 202–206 °C). ¹H NMR (300 MHz, DMSO-*d*₆) (δ/ppm): 14.17–13.55 (1H, m, NH), 10.66 (2H, s, CNH), 8.45–8.26 (2H, m, H5'; H4), 8.20–8.05 (2H, m, Ph; H6), 7.92–7.72 (2H, m, Ph; H7), 7.60 (1H, t, *J* = 8.6 Hz, Ph), 5.36 (2H, s, OCH₂), 4.52 (2H, t, *J* = 6.1 Hz, CH₂CH₂), 4.02 (4H, s, CH₂CH₂), 3.60–3.41 (4H, m, CH₂-morpholine), 2.75 (2H, t, *J* = 5.5 Hz, CH₂CH₂), 2.41 (4H, bs, CH₂-morpholine). ¹³C NMR (75 MHz, DMSO-*d*₆) (δ/ppm): 165.4 (CNH), 153.3 (C2), 153.2; 150.1 (d, *J*_{CF} = 244.1 Hz, Ph-q), 148.0; 147.9 (d, *J*_{CF} = 6.1 Hz, Ph-q), 141.6 (C4'), 125.4 (C5'), 123.9 (Ph), 122.5; 122.4 (d, *J*_{CF} = 7.2 Hz, Ph-q), 115.8 (Ph), 115.7 (C4), 115.3 (C5), 114.7; 114.5 (d, *J*_{CF} = 17.3 Hz, Ph), 112.2 (C7), 66.0 (CH₂-morpholine), 62.2 (OCH₂), 57.2 (CH₂CH₂), 52.9 (CH₂-morpholine), 46.5 (CH₂CH₂), 44.3 (CH₂CH₂). Anal. calcd. for C₂₅H₂₇FN₈O₂ × 2HCl × 2.25H₂O (*M*_r = 603.99): C 49.71, H 5.59, N 18.85; found: C 49.48, H 5.37, N 18.96.

5-(Imidazolin-2-yl)-2-{4-[(1-(2-morpholinoethyl)-1*H*-1,2,3-triazol-4-yl)methoxy]-3-methoxyphenyl}-1*H*-benzo[*d*]imidazole dihydrochloride (7c)

According to the above-mentioned procedure, from compound **3c** (150 mg; 0.43 mmol) compound **7c** was obtained as grey solid (184.1 mg, 85%, m.p. = 180–184 °C). ¹H NMR (600 MHz, DMSO-*d*₆) (δ/ppm): 13.94–13.44 (1H, m, NH), 10.60 (2H, m, CNH), 8.42–8.18 (2H, m, H5', H4), 7.98–7.70 (4H, m, Ph; H6; H7), 7.36 (1H, d, *J* = 8.4 Hz, Ph), 5.24 (2H, s, OCH₂), 4.52 (2H, t, *J* = 5.6 Hz, CH₂CH₂), 4.02 (4H, s, CH₂CH₂), 3.89 (3H, s, OCH₃), 3.53 (4H, s, CH₂-morpholine), 2.75 (2H, s, CH₂CH₂), 2.42 (4H, s, CH₂-morpholine). ¹³C NMR (151 MHz, DMSO-*d*₆) (δ/ppm): 164.8 (CNH), 153.0 (Ph-q), 150.9 (C5), 149.2 (Ph-q), 142.4 (C4'), 125.5 (Ph), 124.1 (C6), 121.6 (C5'), 117.2 (C5), 115.6 (C4), 113.5 (Ph, C7), 111.4 (Ph), 63.0 (CH₂-morpholine), 61.7 (OCH₂), 56.1 (OCH₃), 54.1 (CH₂CH₂), 51.2 (CH₂-morpholine), 44.3 (CH₂CH₂), 43.6 (CH₂CH₂). Anal. calcd. for C₂₆H₃₀N₈O₃ × 2HCl × H₂O (*M*_r = 593.51): C 52.62, H 5.77, N 18.88; found: C 52.29, H 5.94, N 18.73.

4.2.6. General procedure for the synthesis of benzaldehydes 9a–13a, 9b–13b and 9c–13c

The corresponding Hydroxybenzaldehyde (**1a–1c**) was dissolved in dry acetonitrile (15–20 mL) and K_2CO_3 (1.5 eq) was added. The reaction mixture was stirred for 30 min and the appropriate halide (1 eq) was added and stirring was continued overnight at reflux temperature. The course of the reaction was monitored by TLC. After completion of the reaction, the solvent was evaporated under reduced pressure and the residue was purified by column chromatography.

4-(2-Morpholino-2-oxoethoxy)benzaldehyde (9a)

Compound **9a** was prepared according to the general procedure from 4-hydroxybenzaldehyde **1a** (250 mg, 2.05 mmol) and *N*-(chloroacetyl)morpholine (0.27 mL, 2.05 mmol). After purification with column chromatography (CH_2Cl_2 : CH_3OH = 100 : 1) compound **9a** was obtained as white solid (506.7 mg, 99%, m.p. = 147–150 °C). 1H NMR (300 MHz, $DMSO-d_6$) (δ/ppm): 9.87 (1H, s, CHO), 7.85 (2H, d, J = 8.8 Hz, Ph), 7.11 (2H, d, J = 8.7 Hz, Ph), 5.01 (2H, s, OCH_2), 3.68–3.52 (4H, m, CH_2 -morpholine), 3.51–3.40 (4H, m, CH_2 -morpholine). ^{13}C NMR (75 MHz, $DMSO-d_6$) (δ/ppm): 191.3 (CHO), 165.4 (CO), 163.1 (Ph-q), 131.6 (Ph), 129.8 (Ph-q), 115.1 (Ph), 66.0 (CH_2 -morpholine), 65.6 (OCH_2), 44.6 (CH_2 -morpholine), 41.6 (CH_2 -morpholine).

3-Fluoro-4-(2-morpholino-2-oxoethoxy)benzaldehyde (9b)

Compound **9b** was prepared according to the general procedure from 3-fluoro-4-hydroxybenzaldehyde **1b** (250 mg, 1.78 mmol) and *N*-(chloroacetyl)morpholine (0.23 mL, 1.78 mmol). After purification with column chromatography (CH_2Cl_2 : CH_3OH = 50 : 1) compound **9b** was obtained as white solid (473.9 mg, 99%, m.p. = 84–88 °C). 1H NMR (300 MHz, $DMSO-d_6$) (δ/ppm): 9.86 (1H, d, J = 2.0 Hz, CHO), 7.80–7.67 (2H, m, Ph), 7.28 (1H, t, J = 8.5 Hz, Ph), 5.13 (2H, s, OCH_2), 3.64–3.54 (4H, m, CH_2 -morpholine), 3.47–3.42 (4H, m, CH_2 -morpholine). ^{13}C NMR (75 MHz, $DMSO-d_6$) (δ/ppm): 190.8; 190.8 (d, J_{CF} = 1.9 Hz, CHO), 165.0 (CO), 153.2; 149.9 (d, J_{CF} = 247.0 Hz, Ph-q) 151.4; 151.3 (d, J_{CF} = 10.5 Hz, Ph-q), 129.9; 129.8 (d, J_{CF} = 5.2 Hz, Ph-q), 127.8; 127.8 (d, J_{CF} = 2.9 Hz, Ph), 115.5; 115.3 (d, J_{CF} = 18.3 Hz, Ph), 115.0; 115.0 (d, J_{CF} = 1.5 Hz), 66.1 (CH_2 -morpholine), 65.9 (OCH_2), 44.5 (CH_2 -morpholine), 41.6 (CH_2 -morpholine).

3-Methoxy-4-(2-morpholino-2-oxoethoxy)benzaldehyde (9c)

Compound **9c** was prepared according to the general procedure from 3-methoxy-4-hydroxybenzaldehyde **1c** (250 mg, 1.64 mmol) and *N*-(chloroacetyl)morpholine (0.21 mL, 1.64 mmol). After purification with column chromatography (CH_2Cl_2 : CH_3OH = 50 : 1) compound

9c was obtained as white solid (452.3 mg, 99%, m.p. = 80–85 °C). ¹H NMR (300 MHz, DMSO-*d*₆) (δ/ppm): 9.84 (1H, s, CHO), 7.51 (1H, dd, *J* = 8.3, 1.9 Hz, Ph), 7.42 (1H, d, *J* = 1.8 Hz, Ph), 7.06 (1H, d, *J* = 8.3 Hz, Ph), 5.0 (2H, s, OCH₂), 3.85 (3H, s, OCH₃), 3.71–3.52 (4H, m, CH₂-morpholine), 3.50–3.39 (4H, m, CH₂-morpholine). ¹³C NMR (75 MHz, DMSO-*d*₆) (δ/ppm): 191.4 (CHO), 165.3 (CO), 152.9 (Ph-q), 149.2 (Ph-q), 129.9 (Ph-q), 125.5 (Ph), 112.7 (Ph), 110.0 (Ph), 66.1 (OCH₂, CH₂-morpholine), 55.6 (OCH₃), 44.7 (CH₂-morpholine), 41.6 (CH₂-morpholine).

4-(2-Oxo-2-phenylethoxy)benzaldehyde (10a)

Compound **10a** was prepared according to the general procedure from 4-hydroxybenzaldehyde **1a** (250 mg, 2.5 mmol) and 2-bromoacetophenone (352.4 mg, 1.78 mmol). After purification with column chromatography (CH₂Cl₂ : CH₃OH = 50 : 1) compound **10a** was obtained as yellow solid (324.7 mg, 71%, m.p. = 81–85 °C). ¹H NMR (300 MHz, DMSO-*d*₆) (δ/ppm): 9.87 (1H, s, CHO), 8.04 (2H, d, *J* = 7.1 Hz, Ph), 7.86 (2H, d, *J* = 8.8 Hz, Ph), 7.71 (1H, t, *J* = 7.4 Hz, Ph), 7.58 (2H, t, *J* = 7.5 Hz, Ph), 7.17 (2H, d, *J* = 8.7 Hz, Ph), 5.77 (2H, s, OCH₂). ¹³C NMR (151 MHz, DMSO-*d*₆) (δ/ppm): 193.7 (CO), 191.2 (CHO), 162.9 (Ph-q), 134.2 (Ph-q), 133.8 (Ph), 131.6 (Ph), 129.9 (Ph-q), 128.8 (Ph), 127.8 (Ph), 115.1 (Ph), 70.3 (OCH₂).

3-Fluoro-4-(2-oxo-2-phenylethoxy)benzaldehyde (10b)

Compound **10b** was prepared according to the general procedure from 3-fluoro-4-hydroxybenzaldehyde **1b** (250 mg, 1.78 mmol) and 2-bromoacetophenone (322.4 mg, 1.78 mmol). After purification with column chromatography (CH₂Cl₂ : CH₃OH = 50 : 1) compound **10b** was obtained as yellow solid (365.9 mg, 72%, m.p. = 115–120 °C). ¹H NMR (300 MHz, DMSO-*d*₆) (δ/ppm): 9.86 (1H, d, *J* = 2.0 Hz, CHO), 8.06–7.89 (2H, m, Ph), 7.83–7.65 (3H, m, Ph), 7.59 (2H, t, *J* = 7.6 Hz, Ph), 7.35 (1H, t, *J* = 8.5 Hz, Ph), 5.89 (2H, s, OCH₂). ¹³C NMR (75 MHz, DMSO-*d*₆) (δ/ppm): 193.4 (CO), 190.8; 190.8 (d, *J*_{CF} = 1.8 Hz, CHO), 153.2; 149.9 (d, *J*_{CF} = 247.1 Hz, Ph-q), 151.3; 151.1 (d, *J*_{CF} = 10.6 Hz, Ph-q), 134.0 (Ph), 130.0; 129.9 (d, *J*_{CF} = 5.0 Hz, Ph-q), 128.9 (Ph), 128.0 (Ph), 127.9 (Ph), 115.6 (Ph), 115.4; 115.1 (d, *J*_{CF} = 18.3 Hz, Ph), 115.0 (Ph), 70.9 (OCH₂).

3-Methoxy-4-(2-oxo-2-phenylethoxy)benzaldehyde (10c)

Compound **10c** was prepared according to the general procedure from 3-methoxy-4-hydroxybenzaldehyde **1c** (250 mg, 1.64 mmol) and 2-bromoacetophenone (324.7 mg, 1.64 mmol). After purification with column chromatography (CH₂Cl₂ : CH₃OH = 50 : 1) compound

10c was obtained as white solid (424.7 mg, 96%, m.p. = 132–134 °C). ¹H NMR (300 MHz, DMSO-*d*₆) (δ/ppm): 9.84 (1H, s, CHO), 8.03 (2H, d, *J* = 7.2 Hz, Ph), 7.70 (1H, d, *J* = 7.4 Hz, Ph), 7.58 (2H, t, *J* = 7.5 Hz, Ph), 7.52–7.40 (2H, m, Ph), 7.10 (1H, d, *J* = 8.3 Hz, Ph), 5.77 (2H, s, OCH₂), 3.88 (3H, s, OCH₃). ¹³C NMR (151 MHz, DMSO-*d*₆) (δ/ppm): 193.7 (CO), 191.3 (CHO), 152.8 (Ph-q), 149.2 (Ph-q), 134.2 (Ph-q), 133.9 (Ph), 130.0 (Ph-q), 128.8 (Ph), 127.9 (Ph), 125.5 (Ph), 112.7 (Ph), 110.1 (Ph), 70.5 (OCH₂), 55.6 (OCH₃).

4-(Piridin-2-yl-methoxy)benzaldehyde (11a)

Compound **11a** was prepared according to the general procedure from 4-hydroxybenzaldehyde **1a** (250 mg, 2.5 mmol) and 2-(chloromethyl)pyridine (403.5 mg, 2.05 mmol). After purification with column chromatography (CH₂Cl₂ : CH₃OH = 100 : 1) compound **11a** was obtained as white solid (385.3 mg, 88%, m.p. = 94–97 °C). ¹H NMR (300 MHz, DMSO-*d*₆) (δ/ppm): 9.87 (1H, s, CHO), 8.59 (1H, d, *J* = 4.2 Hz, H6'), 7.92–7.80 (3H, m, Ph, H4'), 7.53 (1H, d, *J* = 7.8 Hz, H3'), 7.36 (1H, dd, *J* = 6.8, 5.0 Hz, H5'), 7.23 (2H, d, *J* = 8.7 Hz, Ph), 5.31 (2H, s, OCH₂). ¹³C NMR (75 MHz, DMSO-*d*₆) (δ/ppm): 191.3 (CHO), 163.1 (Ph-q), 155.9 (C2'), 149.2 (C6'), 137.1 (Ph), 131.8 (Ph-q), 129.9 (C4'), 123.2 (C3'), 121.9 (C5'), 115.3 (Ph), 70.6 (OCH₂).

3-Fluoro-4-(piridin-2-yl-methoxy)benzaldehyde (11b)

Compound **11b** was prepared according to the general procedure from 3-fluoro-4-hydroxybenzaldehyde **1b** (250 mg, 1.78 mmol) and 2-(chloromethyl)pyridine (351.0 mg, 1.78 mmol). After purification with column chromatography (CH₂Cl₂ : CH₃OH = 100 : 1) compound **11b** was obtained as white solid (307.6 mg, 75%, m.p. = 82–85 °C). ¹H NMR (300 MHz, DMSO-*d*₆) (δ/ppm): 9.87 (1H, d, *J* = 2.1 Hz, CHO), 8.76–8.33 (1H, m, 6'), 7.87 (1H, td, *J* = 7.7, 1.8 Hz, Ph), 7.80–7.70 (2H, m, Ph, H4'), 7.55 (1H, d, *J* = 7.8 Hz, H3'), 7.47 (1H, t, *J* = 8.2 Hz, Ph), 7.41–7.32 (1H, m, H5'), 5.39 (2H, s, OCH₂). ¹³C NMR (151 MHz, DMSO-*d*₆) (δ/ppm): 190.8 (CHO), 155.3 (Ph-q, C2') 152.5; 150.8 (d, *J*_{CF} = 246.9 Hz, Ph-q), 151.3; 151.2 (d, *J*_{CF} = 10.5 Hz, Ph-q), 149.2 (C6'), 137.1 (Ph), 130.0; 129.9 (d, *J*_{CF} = 5.1 Hz, Ph-q), 128.2 (C4'), 123.3 (C5'), 121.9 (C5'), 115.4; 115.3 (d, *J*_{CF} = 18.2 Hz, Ph), 115.1 (Ph), 71.3 (OCH₂).

3-Methoxy-4-(piridin-2-yl-methoxy)benzaldehyde (11c)

Compound **11c** was prepared according to the general procedure from 3-methoxy-4-hydroxybenzaldehyde **1c** (250 mg, 1.64 mmol) and 2-(chloromethyl)pyridine (323.14 mg, 1.64 mmol). After purification with column chromatography (CH₂Cl₂ : CH₃OH = 100 : 1) compound

11c was obtained as white solid (398.67 mg, 60%, m.p. = 77–81 °C). ¹H NMR (300 MHz, DMSO-*d*₆) (δ/ppm): 9.85 (1H, s, CHO), 8.59 (1H, d, *J* = 4.2 Hz, H6'), 7.86 (1H, td, *J* = 7.7, 1.7 Hz, Ph), 7.58–7.48 (2H, m, H4', H3'), 7.44 (1H, d, *J* = 1.8 Hz, Ph), 7.37 (1H, dd, *J* = 6.8, 5.1 Hz, H5'), 7.26 (1H, d, *J* = 8.3 Hz, Ph), 5.29 (2H, s, OCH₂), 3.87 (3H, s, OCH₃). ¹³C NMR (151 MHz, DMSO-*d*₆) (δ/ppm): 191.4 (CHO), 155.9 (Ph-q), 152.9 (Ph-q), 149.4 (C2'), 149.2 (C6'), 137.1 (Ph), 130.0 (Ph-q), 125.8 (C4'), 123.2 (C3'), 121.9 (C5'), 112.7 (Ph), 109.9 (Ph), 70.9 (OCH₂), 55.6 (OCH₃).

4-(2-Morpholinoethoxy)benzaldehyde (**12a**)

Compound **12a** was prepared according to the general procedure from 4-hydroxybenzaldehyde **1a** (250 mg, 2.5 mmol) and 4-(2-chloroethyl)morpholine hydrochloride (340 mg, 2.05 mmol). After purification with column chromatography (CH₂Cl₂ : CH₃OH = 50 : 1) compound **12a** was obtained as colourless oil (425.2 mg, 88%). ¹H NMR (300 MHz, DMSO-*d*₆) (δ/ppm): 9.86 (1H, s, CHO), 7.85 (2H, d, *J* = 8.8 Hz, Ph), 7.13 (2H, d, *J* = 8.7 Hz, Ph), 4.20 (2H, t, *J* = 5.7 Hz, CH₂CH₂), 3.70–3.47 (4H, m, CH₂-morpholine), 2.71 (2H, t, *J* = 5.7 Hz, CH₂CH₂), 2.49–2.43 (4H, m, CH₂-morpholine). ¹³C NMR (151 MHz, DMSO-*d*₆) (δ/ppm): 191.3 (CHO), 163.4 (Ph-q), 131.2 (Ph), 129.6 (Ph-q), 115.0 (Ph), 66.1 (CH₂-morpholine), 65.8 (CH₂CH₂), 56.8 (CH₂CH₂), 53.5 (CH₂-morpholine).

3-Fluoro-4-(2-morpholinoethoxy)benzaldehyde (**12b**)

Compound **12b** was prepared according to the general procedure from 3-fluoro-4-hydroxybenzaldehyde **1b** (250 mg, 1.78 mmol) and 4-(2-chloroethyl)morpholine hydrochloride (331.22 mg, 1.78 mmol). After purification with column chromatography (CH₂Cl₂ : CH₃OH = 50 : 1) compound **12b** was obtained as yellow oil (430.4 mg, 95%). ¹H NMR (300 MHz, DMSO-*d*₆) (δ/ppm): 9.86 (1H, d, *J* = 2.1 Hz, CHO), 7.79–7.74 (1H, m, Ph), 7.68 (1H, dd, *J* = 11.4, 1.9 Hz, Ph), 7.41 (1H, t, *J* = 8.3 Hz, Ph), 4.29 (2H, t, *J* = 5.7 Hz, CH₂CH₂), 3.64–3.46 (4H, m, CH₂-morpholine), 2.74 (2H, t, *J* = 5.7 Hz, CH₂CH₂), 2.49–2.43 (4H, m, CH₂-morpholine). ¹³C NMR (75 MHz, DMSO-*d*₆) (δ/ppm): 190.8 (CHO), 153.3; 150.0 (d, *J*_{CF} = 246.9 Hz, Ph-q), 151.8; 151.6 (d, *J*_{CF} = 10.7 Hz, Ph-q), 129.7; 129.6 (d, *J*_{CF} = 4.9 Hz, Ph-q), 128.3; 128.3 (d, *J*_{CF} = 3.1 Hz, Ph), 115.3; 115.1 (d, *J*_{CF} = 18.3 Hz, Ph), 114.7; 114.7 (d, *J*_{CF} = 1.6 Hz, Ph), 67.0 (CH₂-morpholine), 66.1 (CH₂CH₂), 56.6 (CH₂CH₂), 53.5 (CH₂-morpholine).

3-Methoxy-4-(2-morpholinoethoxy)benzaldehyde (**12c**)

Compound **12c** was prepared according to the general procedure from 3-methoxy-4-hydroxybenzaldehyde **1c** (250 mg, 1.64 mmol) and 4-(2-chloroethyl)morpholine hydrochloride (305.17 mg, 1.64 mmol). After purification with column chromatography (CH₂Cl₂ : CH₃OH = 50 : 1) compound **12c** was obtained as yellow oil (415.9 mg, 96%). ¹H NMR (300 MHz, DMSO-*d*₆) (δ/ppm): 9.84 (1H, s, CHO), 7.53 (1H, dd, *J* = 8.2, 1.9 Hz, Ph), 7.39 (1H, d, *J* = 1.8 Hz, Ph), 7.20 (1H, d, *J* = 8.3 Hz, Ph), 4.19 (2H, t, *J* = 5.9 Hz, CH₂CH₂), 3.83 (3H, s, OCH₃), 3.62–3.45 (4H, m, CH₂-morpholine), 2.72 (2H, t, *J* = 5.8 Hz, CH₂CH₂), 2.49–2.43 (4H, m, CH₂-morpholine). ¹³C NMR (75 MHz, DMSO-*d*₆) (δ/ppm): 191.4 (CHO), 153.4 (Ph-q), 149.3 (Ph-q), 129.7 (Ph-q), 126.0 (Ph), 112.3 (Ph), 109.7 (Ph), 66.4 (CH₂CH₂), 66.2 (CH₂-morpholine), 56.8 (CH₂CH₂), 55.6 (OCH₃), 53.6 (CH₂-morpholine).

4-(2-(Diethylamino)ethoxy)benzaldehyde (**13a**)

Compound **13a** was prepared according to the general procedure from 4-hydroxybenzaldehyde **1a** (250 mg; 2,5 mmol) and 2-chloro-*N,N*-dimethylethylamine hydrochloride (339.42 mg, 2.05 mmol). After purification with column chromatography (CH₂Cl₂ : CH₃OH = 50 : 1) compound **13a** was obtained as yellow oil (136.4 mg, 30%). ¹H NMR (300 MHz, DMSO-*d*₆) (δ/ppm): 9.86 (1H, s, CHO), 7.85 (2H, d, *J* = 8.8 Hz, Ph), 7.12 (2H, d, *J* = 8.7 Hz, Ph), 4.14 (2H, t, *J* = 6.0 Hz, CH₂CH₂), 2.81 (2H, t, *J* = 5.9 Hz, CH₂CH₂) 2.62–2.51 (4H, m, CH₂CH₃), 0.97 (6H, t, *J* = 7.1 Hz, CH₂CH₃). ¹³C NMR (75 MHz, DMSO-*d*₆) (δ/ppm): 191.8 (CHO), 164.0 (Ph-q), 132.3 (Ph), 130.0 (Ph-q), 115.4 (Ph), 67.3 (CH₂CH₂), 51.6 (CH₂CH₂), 47.4 (CH₂CH₃), 12.2 (CH₂CH₃).

4-(2-(Diethylamino)ethoxy)-3-fluorobenzaldehyde (**13b**)

Compound **13b** was prepared according to the general procedure from 3-fluoro-4-hydroxybenzaldehyde **1b** (250 mg, 1.78 mmol) and 2-chloro-*N,N*-dimethylethylamine hydrochloride (295.87 mg, 1.78 mmol). After purification with column chromatography (CH₂Cl₂ : CH₃OH = 50 : 1) compound **13b** was obtained as yellow oil (335.1 mg, 79%). ¹H NMR (300 MHz, DMSO-*d*₆) (δ/ppm): 9.82 (1H, d, *J* = 2.1 Hz, CHO), 7.72 (1H, d, *J* = 8.5 Hz, Ph), 7.64 (1H, dd, *J* = 11.4, 1.9 Hz, Ph), 7.37 (1H, t, *J* = 8.3 Hz, Ph), 4.17 (2H, t, *J* = 5.9 Hz, CH₂CH₂), 2.92–2.70 (2H, m, CH₂CH₂), 2.48–2.41 (4H, m, CH₂CH₃), 0.93 (6H, t, *J* = 7.1 Hz, CH₂CH₃). ¹³C NMR (151 MHz, DMSO-*d*₆) (δ/ppm): 190.7 (CHO), 152.5; 150.8 (d, *J*_{CF} = 247.0 Hz, Ph-q), 151.8; 151.7 (d, *J*_{CF} = 10.7 Hz, Ph-q), 129.6; 129.5 (d, *J*_{CF} = 5.1 Hz, Ph-q), 128.2; 128.2 (d,

$J_{CF} = 2.7$ Hz, Ph), 116.1; 116.0 (, $J_{CF} = 18.3$ Hz, Ph), 114.6 (Ph), 67.8 (CH₂CH₂), 50.9 (CH₂CH₂), 47.0 (CH₂CH₃), 11.7 (CH₂CH₃).

4-(2-(Dietihylamino)ethoxy)-3-methoxybenzaldehyde (13c)

Compound **13c** was prepared according to the general procedure from 3-methoxy-4-hydroxybenzaldehyde **1c** (250 mg; 1.64 mmol) and 2-chloro-*N,N*-dimethylethylamine hydrochloride (271.98 mg, 1.64 mmol). After purification with column chromatography (CH₂Cl₂ : CH₃OH = 50 : 1) compound **13c** was obtained as yellow oil (354.2 mg, 66%). ¹H NMR (300 MHz, DMSO-*d*₆) (δ /ppm): 9.83 (1H, s, CHO), 7.53 (1H, dd, $J = 8.2, 1.9$ Hz, Ph), 7.39 (1H, d, $J = 1.8$ Hz, Ph), 7.19 (1H, d, $J = 8.3$ Hz, Ph), 4.12 (2H, t, $J = 6.2$ Hz, CH₂CH₂), 3.82 (3H, s, OCH₃), 2.81 (2H, t, $J = 6.2$ Hz, CH₂CH₂), 2.66–2.50 (4H, m, CH₂CH₃), 0.97 (6H, t, $J = 7.1$ Hz, CH₂CH₃). ¹³C NMR (75 MHz, DMSO-*d*₆) (δ /ppm): 191.4 (CHO), 153.5 (Ph-q), 149.3 (Ph-q), 129.6 (Ph-q), 126.1 (Ph), 112.2 (Ph), 109.7 (Ph), 67.3 (CH₂CH₂), 55.6 (OCH₃), 51.1 (CH₂CH₂), 47.0 (CH₂CH₃), 11.8 (CH₂CH₃).

4.2.7. General procedure for the synthesis of benzimidazole derivatives **14a–18a**, **14b–18b** and **14c–18c**

The reaction mixture of the corresponding benzaldehyde derivative (**9a–13a**, **9b–13b**, **9c–13c**), 4-(imidazolin-2-yl)benzene-1,2-diamine (1 eq) and 40% NaHSO₃ (aq) was dissolved in 15 ml EtOH and stirred under reflux for 6–8 h. After completion of the reaction NaHSO₃ was filtered and the reaction mixture was evaporated to dryness. The crude residue was purified by column chromatography (CH₂Cl₂ : CH₃OH = 4 : 1). The obtained solid was dissolved in HCl saturated EtOH (8–10 mL) and stirred for 4 h. Addition of ether resulted in precipitation of products **14a–18a**, **14b–18b** and **14c–18c**. Solid was collected by filtration, washed with anhydrous ether, and dried under vacuum.

5-(Imidazolin-2-yl)-2-[4-(2-morpholino-2-oxoethoxy)phenyl]-1*H*-benzo[*d*]imidazole dihydrochloride (14a)

According to the above-mentioned procedure, from **9a** (200 mg, 0.80 mmol) compound **14a** was obtained as brown solid (118.6 mg, 37%, m.p. = 220–223 °C). ¹H NMR (300 MHz, DMSO-*d*₆) (δ /ppm): 10.82 (2H, s, CNH), 8.45 (1H, s, H4), 8.39 (2H, d, $J = 8.5$ Hz, Ph), 8.00 (1H, d, $J = 8.3$ Hz, H7), 7.89 (1H, d, $J = 8.5$ Hz, H6), 7.20 (2H, d, $J = 8.9$ Hz, Ph), 5.01 (2H, s, CH₂), 4.03 (4H, s, CH₂CH₂), 3.73–3.35 (8H, m, CH₂-morpholine). ¹³C NMR (75 MHz, DMSO-*d*₆)

(δ /ppm): 165.6 (CNH), 165.1 (CO), 161.3 (Ph-q), 153.5 (C2), 129.5 (Ph), 123.7 (C6), 118.9 (C5), 116.8 (Ph-q), 115.9 (C4), 115.5 (Ph), 114.8 (C7), 66.1 (CH₂-morpholine), 65.7 (OCH₂), 44.4 (CH₂CH₂), 44.6 (CH₂-morpholine), 41.6 (CH₂-morpholine). Anal. calcd. for C₂₂H₂₃N₅O₃ × 2HCl × 2.75H₂O (M_r = 527.91): C 50.05, H 5.82, N 13.27; found: C 50.28, H 5.94, N 13.11.

2-[3-Fluoro-4-(2-morpholino-2-oxoethoxy)phenyl]-5-(imidazolin-2-yl)-1H-benzo[d]imidazole dihydrochloride (14b)

According to the above-mentioned procedure, from **9b** (200 mg, 0.74 mmol) compound **14b** was obtained as brown solid (265.4 mg, 85%, m.p. = 211–215 °C). ¹H NMR (300 MHz, DMSO-*d*₆) (δ /ppm): 13.87 (1H, s, NH), 10.67 (2H, s, CNH), 8.36 (1H, s, H4), 8.17–8.01 (2H, m, H6, Ph), 7.91–7.72 (2H, m, H7, Ph), 7.29 (1H, t, J = 8.7 Hz, Ph), 5.09 (2H, s, OCH₂), 4.01 (4H, s, CH₂CH₂), 3.69–3.40 (8H, m, CH₂-morpholine). ¹³C NMR (151 MHz, DMSO-*d*₆) (δ /ppm): 165.4 (CNH), 165.3 (CO), 152.2; 150.6 (d, J_{CF} = 244.3 Hz, Ph-q), 149.7 (Ph-q), 148.1; 148.1 (d, J_{CF} = 10.2 Hz, Ph-q), 123.7 (Ph, C6), 122.4; 122.3 (d, J_{CF} = 7.1 Hz, Ph-q), 115.6 (C4, Ph), 115.5 (C5), 115.3 (C7), 114.6; 114.5 (d, J_{CF} = 20.9 Hz, Ph), 66.1 (CH₂-morpholine), 65.9 (OCH₂), 44.6 (CH₂-morpholine), 44.2 (CH₂CH₂), 41.6 (CH₂-morpholine). Anal. calcd. for C₂₂H₂₂FN₅O₃ × 2HCl × 3H₂O (M_r = 550.41): C 48.01, H 5.49, N 12.72; found: C 47.79, H 5.31, N 13.02.

5-(Imidazolin-2-yl)-2-[3-methoxy-4-(2-morpholino-2-oxoethoxy)phenyl]-1H-benzo[d]imidazole dihydrochloride (14c)

According to the above-mentioned procedure, from **9c** (200 mg, 0.72 mmol) compound **14c** was obtained as brown solid (269.7 mg, 86%, m.p. = 202–205 °C). ¹H NMR (300 MHz, DMSO-*d*₆) (δ /ppm): 13.78 (1H, bs, NH), 10.67 (2H, s, CNH), 8.36 (1H, s, H4), 8.00–7.70 (4H, m, Ph; H7; H6), 7.07 (1H, d, J = 8.6 Hz, Ph), 4.94 (2H, s, OCH₂), 4.01 (4H, s, CH₂CH₂), 3.92 (3H, s, OCH₃), 3.73–3.40 (8H, m, CH₂-morpholine). ¹³C NMR (75 MHz, DMSO-*d*₆) (δ /ppm): 165.7 (CNH), 165.4 (Ph-q), 149.7 (C2), 149.0 (Ph-q), 122.3 (C6), 122.2 (Ph-q), 119.9 (Ph), 115.6 (C4, C7), 115.0 (Ph-q), 113.4 (Ph), 110.7 (Ph), 66.3 (CH₂-morpholine), 66.0 (OCH₂), 55.9 (OCH₃), 44.8 (CH₂CH₂), 44.2 (CH₂-morpholine), 41.6 (CH₂-morpholine). Anal. calcd. for C₂₃H₂₅N₅O₄ × 2HCl × 2.25H₂O (M_r = 548.93): C 50.32, H 5.78, N 12.76; found: C 50.47, H 5.43, N 13.11.

5-(Imidazolin-2-yl)-2-[4-(2-oxoethoxy-2-phenyl)phenyl]-1H-benzo[d]imidazole hydrochloride (15a)

According to the above-mentioned procedure, from **10a** (150 mg, 0.62 mmol) compound **15a** was obtained as brown solid (205.0 mg, 83%, m.p. = 255–258 °C). ¹H NMR (300 MHz, DMSO-*d*₆) (δ/ppm): 13.67 (1H, s, NH), 10.62 (2H, s, CNH), 8.33 (1H, s, H4), 8.22 (2H, d, *J* = 8.6 Hz, Ph), 8.06 (2H, d, *J* = 7.2 Hz, Ph), 7.88–7.65 (3H, m, H6; H7; Ph), 7.59 (2H, t, *J* = 7.5 Hz, Ph), 7.19 (2H, d, *J* = 8.9 Hz, Ph), 5.73 (2H, s, OCH₂), 4.01 (4H, s, CH₂CH₂). ¹³C NMR (75 MHz, DMSO-*d*₆) (δ/ppm): 194.2 (CO), 165.4 (CNH), 160.1 (C2), 134.3 (Ph-q), 133.9 (Ph), 128.9 (Ph), 128.7 (Ph), 127.9 (Ph), 122.2 (C6), 122.0 (C5), 115.2 (C4, C7), 115.0 (Ph-q), 70.3 (OCH₂), 44.2 (CH₂CH₂). Anal. calcd. for C₂₄H₂₀N₄O₂ × HCl × 2H₂O (*M*_r = 468.93): C 61.47, H 5.37, N 11.95; found: C 61.09, H 4.98, N 12.30.

2-[3-Fluoro-4-(2-oxoethoxy-2-phenyl)phenyl]-5-(imidazolin-2-yl)-1*H*-benzo[*d*]imidazole hydrochloride (15b)

According to the above-mentioned procedure, from **10b** (150 mg, 0.66 mmol) compound **15b** was obtained as yellow solid (187.2 mg, 68%, m.p. = 205–208 °C). ¹H NMR (300 MHz, DMSO-*d*₆) (δ/ppm): 10.91 (2H, s, CNH), 8.48 (1H, s, H4), 8.39 (1H, dd, *J* = 12.3, 1.9 Hz, Ph), 8.25 (1H, d, *J* = 8.8 Hz, H7), 8.09–7.97 (3H, m, Ph;H6), 7.91 (1H, d, *J* = 8.6 Hz, Ph), 7.72 (1H, t, *J* = 7.4 Hz, Ph), 7.60 (2H, t, *J* = 7.5 Hz, Ph), 7.47 (1H, t, *J* = 8.8 Hz, Ph), 5.90 (2H, s, OCH₂), 4.02 (4H, s, CH₂CH₂). ¹³C NMR (75 MHz, DMSO-*d*₆) (δ/ppm): 193.5 (CO), 165.2 (CNH), 152.9 (C2), 152.9; 149.7 (d, *J*_{CF} = 238.2 Hz, Ph-q), 148.5; 148.3 (d, *J*_{CF} = 10.3 Hz, Ph-q), 134.1 (Ph-q), 133.6 (Ph), 128.6 (Ph), 127.6 (Ph), 124.1; 124.1 (d, *J*_{CF} = 1.3 Hz, Ph), 122.9 (C6), 120.9 (Ph-q), 116.3 (C4), 116.0 (C5), 115.6 (C7), 115.1; 114.8 (d, *J*_{CF} = 20.9 Hz, Ph), 114.8; 114.7 (d, *J*_{CF} = 5.1 Hz, Ph), 70.9 (OCH₂), 44.1 (CH₂CH₂). Anal. calcd. for C₂₄H₁₉FN₄O₂ × HCl × 1.5H₂O (*M*_r = 477.92): C 60.32, H 4.85, N 11.72; found: C 60.03, H 4.98, N 12.07.

2-[3-Fluoro-4-(2-oxoethoxy-2-phenyl)phenyl]-5-(imidazolin-2-yl)-1*H*-benzo[*d*]imidazole hydrochloride (15c)

According to the above-mentioned procedure, from **10c** (150 mg, 0.55 mmol) compound **15c** was obtained as brown solid (183.6 mg, 78%, m.p. = 206–210 °C). ¹H NMR (300 MHz, DMSO-*d*₆) (δ/ppm): 10.66 (2H, s, CNH), 8.34 (1H, s, H4), 8.05 (2H, d, *J* = 7.2 Hz, Ph), 7.97–7.67 (5H, m, Ph), 7.59 (2H, t, *J* = 7.5 Hz, Ph), 7.11 (1H, d, *J* = 8.6 Hz, Ph), 5.71 (2H, s, OCH₂), 4.01 (4H, s, CH₂CH₂), 3.95 (3H, s, OCH₃). ¹³C NMR (75 MHz, DMSO-*d*₆) (δ/ppm): 194.2 (CO), 165.5 (CNH), 153.7 (C2), 149.7 (Ph-q), 149.0 (Ph-q), 134.3 (Ph-q), 133.9 (Ph), 128.9 (Ph), 127.9 (Ph), 122.3 (Ph), 122.0 (Ph), 120.0 (C6), 115.1 (C5), 113.4 (Ph, C7), 110.7 (Ph), 70.6 (OCH₂),

55.9 (OCH₃), 44.2 (CH₂CH₂). Anal. calcd. for C₂₅H₂₂N₄O₃ × HCl × 2.25H₂O (*M_r* = 503.46): C 59.64, H 5.51, N 11.13; found: C 60.06, H 5.21, N 11.37.

5-(Imidazolin-2-yl)-2-[4-(pyridin-2-ylmethoxy)phenyl]-1*H*-benzo[*d*]imidazole hydrochloride (16a)

According to the above-mentioned procedure, from **11a** (150 mg; 0.70 mmol) compound **16a** was obtained as white solid (175.0 mg, 46%, m.p. = 208–211 °C). ¹H NMR (600 MHz, DMSO-*d*₆) (δ/ppm): 11.03 (2H, s, CNH), 8.80 (1H, d, *J* = 4.9 Hz, H6'), 8.54–8.51 (3H, m, H4, Ph), 8.31–8.22 (1H, m, H4'), 8.14–8.07 (1H, m, H6), 7.92 (1H, d, *J* = 8.2 Hz, H7), 7.90 (1H, d, *J* = 7.8 Hz, H3'), 7.73 (1H, dd, *J* = 7.1, 5.1 Hz, H5'), 7.41 (2H, d, *J* = 8.8 Hz, Ph), 5.54 (2H, s, OCH₂), 4.03 (4H, s, CH₂CH₂). ¹³C NMR (75 MHz, DMSO-*d*₆) (δ/ppm): 164.8 (CNH), 161.1 (Ph-q), 154.2 (C2'), 152.8 (C2), 146.8 (C6'), 139.7 (Ph), 138.9 (Ph), 135.3 (Ph-q), 129.9 (C4'), 124.0 (C3'), 123.0 (C5'), 118.53, 117.0 (C5), 115.6 (C4), 115.6 (Ph), 114.4 (C7), 69.0 (OCH₂), 44.2 (CH₂CH₂). Anal. calcd. for C₂₂H₁₉N₅O × HCl × 2H₂O (*M_r* = 441.46): C 59.79, H 5.47, N 15.85; found: C 59.41, H 5.26, N 16.17.

5-(Imidazolin-2-yl)-2-[3-fluoro-4-(pyridin-2-ylmethoxy)phenyl]-1*H*-benzo[*d*]imidazole hydrochloride (16b)

According to the above-mentioned procedure, from **11b** (150 mg, 0.65 mmol) compound **16b** was obtained as brown solid (187.2 mg, 74%, m.p. = 200–203 °C). ¹H NMR (300 MHz, DMSO-*d*₆) (δ/ppm): 10.91 (2H, s, CNH), 8.74 (1H, d, *J* = 4.5 Hz, H6'), 8.48 (1H, s, H4), 8.39 (1H, dd, *J* = 12.3, 1.9 Hz, H6), 8.28 (1H, d, *J* = 8.7 Hz, H7), 8.14 (1H, td, *J* = 7.8, 1.5 Hz, Ph), 8.01 (1H dd, *J* = 8.5, 1.5 Hz, H4'), 7.88 (1H, d, *J* = 8.6 Hz, H3'), 7.79 (1H, d, *J* = 7.9 Hz, Ph), 7.65–7.51 (2H, m, Ph; H5'), 5.52 (2H, s, OCH₂), 4.02 (4H, s, CH₂CH₂). ¹³C NMR (75 MHz, DMSO-*d*₆) (δ/ppm): 165.1 (CNH), 154.9 (C2'), 154.1 (C2), 153.2; 149.9 (d, *J_{CF}* = 245.1 Hz, Ph-q), 152.7 (C2), 148.7; 148.6 (d, *J_{CF}* = 10.5 Hz, Ph-q), 147.4 (C6'), 139.8 (Ph), 136.4 (Ph-q), 124.8; 124.8 (d, *J_{CF}* = 3.1 Hz, Ph), 124.6 (C4'), 124.3 (C3'), 123.5 (C6), 123.1 (C5'), 118.2 (C5), 116.8 (C4), 115.8 (C7), 115.5; 115.2 (d, *J_{CF}* = 21.2 Hz, Ph), 70.0 (OCH₂), 44.4 (CH₂CH₂).). Anal. calcd. for C₂₂H₁₈FN₅O × HCl × 1.75H₂O (*M_r* = 455.40): C 58.02, H 4.98, N 15.38; found: C 57.63, H 5.26, N 15.57.

5-(Imidazolin-2-yl)-2-[3-methoxy-4-(pyridin-2-ylmethoxy)phenyl]-1*H*-benzo[*d*]imidazole hydrochloride (16c)

According to the above-mentioned procedure, from **11c** (150 mg; 0,62 mmol) compound **16c** was obtained as brown solid (181.7 mg; 73%, m.p. = 265–268 °C). ¹H NMR (600 MHz, DMSO-*d*₆) (δ/ppm): 10.67 (2H, s, CNH), 8.60 (1H, d, *J* = 4.6 Hz, H6'), 8.35 (1H, s, H4), 7.96 (1H, s, Ph), 7.92–7.81 (3H, m, Ph; H4'; H6), 7.77 (1H, d, *J* = 8.2 Hz, H7), 7,56 (1H, d, *J* = 7.9 Hz, H3'), 7.37 (1H, dd, *J* = 7.2, 5.1 Hz, H5'), 7.24 (1H, d, *J* = 8.5 Hz, Ph), 5.27 (2H, s, OCH₂), 4.01 (4H, s, CH₂CH₂), 3.94 (3H, s, OCH₃). ¹³C NMR (75 MHz, DMSO-*d*₆) (δ/ppm): 165.4 (CNH), 156.4 (C2), 149.8 (Ph-q), 149.2 (Ph-q), 149.1 (C6'), 137.1 (Ph), 123.1 (C4'), 122.3 (C6), 122.2 (C5), 121.8 (C5'), 120.1 (C3'), 115.1 (Ph-q), 113.4 (C4/C7), 110.6 (Ph), 70.9 (OCH₂), 55.9 (OCH₃), 44.2 (CH₂CH₂). Anal. calcd. for C₂₃H₂₁N₅O₂ × HCl × 3H₂O (*M*_r = 489.95): C 56.38, H 5.76, N 14.29; found: C 56.03, H 5.39, N 14.57.

5-(Imidazolin-2-yl)-2-[4-(2-morpholinoethoxy)phenyl]1-1*H*-benzo[*d*]imidazole hydrochloride (17a)

According to the above-mentioned procedure, from **12a** (150 mg; 0.64 mmol) compound **17a** was obtained as brown solid (248.5 mg, 74%, m.p. = 203–207 °C). ¹H NMR (600 MHz, DMSO-*d*₆) (δ/ppm): 11.82 (1H, s, NH), 10.96 (2H, s, CNH), 8.49–8.44 (3H, m, H4, Ph), 8.04 (1H, dd, *J* = 8.6, 1.3 Hz, H6), 7.89 (1H, d, *J* = 8.6 Hz, H7), 7.28 (2H, d, *J* = 8.9 Hz, Ph), 4.61 (2H, t, *J* = 5.1 Hz, CH₂CH₂), 4.02 (4H, s, CH₂CH₂), 3.96–3.87 (6H, m, CH₂-morpholine, CH₂CH₂), 3.64–3.40 (4H, m, CH₂-morpholine, CH₂CH₂). ¹³C NMR (151 MHz, DMSO-*d*₆) (δ/ppm): 165.2 (CNH), 159.6 (Ph-q), 154.0 (C2), 129.0 (Ph), 122.6 (C6), 121.3 (Ph-q), 115.5 (C5), 115.2 (Ph), 115.0 (C4, C7), 62.9 (CH₂-morpholine), 62.4 (CH₂CH₂), 54.5 (CH₂CH₂), 51.5 (CH₂-morpholine), 44.0 (CH₂CH₂).

5-(Imidazolin-2-yl)-2-[3-fluoro-4-(2-morpholinoethoxy)phenyl]1-1*H*-benzo[*d*]imidazole dihydrochloride (17b)

According to the above-mentioned procedure, from **12b** (150 mg, 0.59 mmol) compound **17b** was obtained as brown solid (301.4 mg, 74%, m.p. = 204–208 °C). ¹H NMR (300 MHz, DMSO-*d*₆) (δ/ppm): 12.00 (1H, bs, NH), 10.99 (2H, s, CNH), 8.50 (1H, s, H4), 8.44–8.25 (2H, m, Ph), 8.04 (1H, dd, *J* = 8.6, 1.4 Hz, H6), 7.86 (1H, d, *J* = 8.6 Hz, H7), 7.53 (1H, t, *J* = 8.7 Hz, Ph), 4.75–4.68 (2H, m, CH₂CH₂), 4.01 (4H, s, CH₂CH₂), 3.98–3.80 (4H, m, CH₂-morpholine), 3.70–3.61 (2H, m, CH₂-morpholine), 3.56–3.45 (2H, m, CH₂-morpholine) 3.33–3.18 (2H, m, CH₂CH₂). ¹³C NMR (75 MHz, DMSO-*d*₆) (δ/ppm): 165.1 (CNH), 153.1; 149.8 (d, *J*_{CF} = 244.9 Hz, Ph-q), 152.8 (C2), 147.8; 147.5 (*J*_{CF} = 10.0 Hz, Ph-q), 124.3; 124.3 (*J*_{CF} = 1.5 Hz, Ph), 122.9 (C6),

121.9; 121.8 ($J_{CF} = 7.5$ Hz, Ph-q), 116.5 (C4), 115.8 (C5), 115.7 (Ph), 115.1; 114.8 (d, $J_{CF} = 20.6$ Hz, Ph), 114.7 (C7), 63.8 (CH₂CH₂), 62.9 (CH₂-morpholine), 54.4 (CH₂CH₂), 51.5 (CH₂-morpholine), 44.0 (CH₂CH₂). Anal. calcd. for C₂₂H₂₄FN₅O₂ × 2HCl × 2.5H₂O ($M_r = 527.42$): C 50.10, H 5.92, N 13.28; found: C 50.03, H 5.71, N 13.72.

5-(Imidazolin-2-yl)-2-[3-methoxy-4-(2-morpholinoethoxy)phenyl]1-*H*-benzo[*d*]imidazole dihydrochloride (17c)

According to the above-mentioned procedure, from **12c** (150 mg; 0,56 mmol) compound **17c** was obtained as yellow solid (237.7 mg, 87%, m.p. = 217–223 °C). ¹H NMR (300 MHz, DMSO-*d*₆) (δ /ppm): ¹H NMR (300 MHz, DMSO) δ 12.08 (1H, bs, NH), 10.97 (2H, s, CNH), 8.50 (1H, s, H4), 8.24 (1H, d, $J = 1.8$ Hz, Ph), 8.15–8.01 (2H, m, Ph, H6), 7.87 (1H, d, $J = 8.6$ Hz, H7), 7.31 (1H, d, $J = 8.6$ Hz, Ph), 4.63 (2H, t, $J = 5.1$ Hz, CH₂CH₂), 4.02 3H, s, OCH₃), 3.97–3.88 (8H, m, CH₂CH₂, CH₂-morpholine), 3.65–3.40 (4H, m, CH₂-morpholine, CH₂CH₂), 3.32–3.20 (2H, m, CH₂-morpholine). ¹³C NMR (151 MHz, DMSO-*d*₆) (δ /ppm): 165.0 (CNH), 153.3 (C2), 149.8 (Ph-q), 149.4 (Ph-q), 123.3 (Ph), 121.0 (C6), 120.5 (Ph-q), 116.2 (C5), 115.9 (C4), 114.4 (Ph, C7), 111.9 (Ph), 63.6 (CH₂CH₂), 62.8 (CH₂-morpholine), 56.2 (OCH₃), 54.5 (CH₂CH₂), 51.5 (CH₂-morpholine), 44.0 (CH₂CH₂). Anal. calcd. for C₂₃H₂₇N₅O₃ × 2HCl × 2H₂O ($M_r = 530.44$): C 52.08, H 6.27, N 13.20; found: C 52.43, H 5.98, N 13.11.

2-{4-[2-(Diethylamino)ethoxy]phenyl}-5-(imidazolin-2-yl)-1-*H*-benzo[*d*]imidazole dihydrochloride (18a)

According to the above-mentioned procedure, from **13a** (150 mg, 0.68 mmol) compound **18a** was obtained as brown solid (126.8 mg, 49%, m.p. = 214–218 °C). ¹H NMR (300 MHz, DMSO-*d*₆) (δ /ppm): 10.98 (3H, s, CNH), 8.54–8.40 (3H, m, Ph, H4), 8.06 (1H, dd, $J = 8.6, 1.3$ Hz, H6), 7.90 (1H, d, $J = 8.6$ Hz, H7), 7.28 (2H, d, $J = 8.9$ Hz, Ph), 4.56 (2H, t, $J = 4.8$ Hz, CH₂CH₂), 4.02 (4H, s, CH₂CH₂), 3.63–3.44 (2H, m, CH₂CH₂), 3.29–3.10 (4H, m, CH₂CH₃), 1.28 (6H, t, $J = 7.2$ Hz, CH₂CH₃). ¹³C NMR (75 MHz, DMSO-*d*₆) (δ /ppm): 164.9 (CNH), 160.6 (Ph-q), 153.2 (C2), 129.8 (Ph), 123.9 (C6), 120.5 (Ph-q), 116.8 (C5), 115.4 (Ph), 114.7 (C4, C7), 62.7 (CH₂CH₂), 49.5 (CH₂CH₂), 46.9 (CH₂CH₃), 44.3 (CH₂CH₂), 8.4 (CH₂CH₃). Anal. calcd. for C₂₂H₂₇N₅O × 2HCl × 3H₂O ($M_r = 504.45$): C 52.38, H 6.99, N 13.88; found: C 52.21, H 6.58, N 14.12.

2-{4-[2-(Diethylamino)ethoxy]-3-fluorophenyl}-5-(imidazolin-2-yl)-1-*H*-benzo[*d*]imidazole dihydrochloride (18b)

According to the above-mentioned procedure, from **13b** (150 mg; 0,63 mmol) compound **18b** was obtained as brown solid (157,0 mg; 63 %, m.p. = 205–207 °C). ¹H NMR (300 MHz, DMSO-*d*₆) (δ/ppm): 11.00 (1H, bs, NH), 10.90 (2H, s, CNH), 8.48 (1H, s, H4), 8.40–8.26 (2H, m, Ph), 8.00 (1H, dd, *J* = 8.6, 1.5 Hz, H6), 7.87 (1H, d, *J* = 8.6 Hz, H7), 7.52 (1H, t, *J* = 8.7 Hz, Ph), 4.64 (2H, t, *J* = 4.8 Hz, CH₂CH₂), 4.02 (4H, s, CH₂CH₂), 3.67–3.52 (2H, m, CH₂CH₂), 3.32–3.14 (4H, m, CH₂CH₃), 1.28 (6H, t, *J* = 7.2 Hz, CH₂CH₃). ¹³C NMR (75 MHz, DMSO-*d*₆) (δ/ppm): 165.1 (CNH), 153.1; 149.8 (d, *J*_{CF} = 245.0 Hz, Ph-q), 152.7 (C2), 148.3; 148.1 (d, *J*_{CF} = 10.7 Hz, Ph-q), 124.8; 124.8 (*J*_{CF} = 1.2 Hz, Ph), 123.4 (C6), 121.1; 121.0 (d, *J*_{CF} = 7.5 Hz, Ph-q), 116.5 (C4), 116.4 (C5), 115.5 (Ph), 115.3; 115.1 (d, *J*_{CF} = 20.7 Hz, Ph), 115.0 (C7), 63.9 (CH₂CH₂), 49.5 (CH₂CH₂), 47.3 (CH₂CH₃), 44.3 (CH₂CH₂), 8.5 (CH₂CH₃). Anal. calcd. for C₂₂H₂₆FN₅O × 2HCl × 1.5H₂O (*M*_r = 495.42): C 53.34, H 6.31, N 14.14; found: C 53.70, H 6.11, N 14.27.

2-{4-[2-(Diethylamino)ethoxy]-3-methoxyphenyl}-5-(imidazolin-2-yl)-1*H*-benzo[*d*]imidazole dihydrochloride (18c)

According to the above-mentioned procedure, from **13c** (150 mg, 0.60 mmol) compound **18b** was obtained as yellow solid (183.0 mg, 75%, m.p. = 227–229 °C). ¹H NMR (300 MHz, DMSO-*d*₆) (δ/ppm): 10.92 (1H, bs, NH), 10.78 (2H, s, CNH), 8.43 (1H, d, *J* = 1.0 Hz, 4H), 8.12 (1H, d, *J* = 1.7 Hz, Ph), 8.01 (1H, dd, *J* = 8.4, 1.8 Hz, Ph), 7.95 (1H, dd, *J* = 8.6, 1.5 Hz, H6), 7.83 (1H, d, *J* = 8.5 Hz, H7), 7.27 (1H, d, *J* = 8.5 Hz, Ph), 4.62–4.36 (2H, m, CH₂CH₂), 4.03 (4H, s, CH₂CH₂), 3.96 (3H, s, OCH₃), 3.59–3.38 (2H, m, CH₂CH₂), 3.32–3.20 (4H, m, CH₂CH₃), 1.30 (6H, t, *J* = 7.2 Hz, CH₂CH₃). ¹³C NMR (75 MHz, DMSO-*d*₆) (δ/ppm): 165.1 (CNH), 153.6 (C2), 149.3 (Ph-q), 123.0 (Ph), 120.8 (C6), 117.3 (C5), 115.9 (C4), 114.5 (C7), 113.9 (Ph), 111.5 (Ph), 63.5 (CH₂CH₂), 56.2 (OCH₃), 49.5 (CH₂CH₂), 47.1 (CH₂CH₃), 44.1 (CH₂CH₂), 8.3 (CH₂CH₃). Anal. calcd. for C₂₃H₂₉N₅O₂ × 2HCl × 2H₂O (*M*_r = 516.46): C 53.49, H 6.83, N 13.56; found: C 53.11, H 6.33, N 13.89.

4.3. Anti-trypanosomal screening and cytotoxicity assays

4.3.1. Anti-trypanosomal screening

Bloodstream form *T. brucei* (strain 221) were grown in modified Iscove's medium, as described [77] and growth inhibition assays were performed using 96-well microtiter plates. The compound concentrations that inhibited growth by 50% (IC₅₀) and 90% (IC₉₀) were determined. Parasites were initially sub-cultured at 2.5 × 10⁴ mL⁻¹, compounds were added at

range of concentrations, and the plates incubated at 37 °C. Resazurin was added after 48 h, the plates incubated for a further 16 h, and then read in a Spectramax plate reader. The data were analysed using GraphPad Prism. Each drug concentration was tested in triplicate.

4.3.2. L6 cell proliferation

For cytotoxicity assays, L6 cells (a rat myoblast line) were seeded into 96-well microtiter plates at $1 \times 10^4 \text{ mL}^{-1}$ in 200 μL of growth medium, and different compound concentrations were added. The plates were then incubated for 6 days at 37 °C and 20 μL resazurin added to each well. After further 8 h incubation, the fluorescence was determined using a Spectramax plate reader, as outlined above.

4.4. DNA and RNA binding study

The UV/vis spectra were recorded on a Varian Cary 100 Bio spectrophotometer, CD spectra on JASCO J815 spectrophotometer and fluorescence spectra on a Varian Cary Eclipse spectrophotometer at 25 °C using appropriate 1cm path quartz cuvettes.

Polynucleotides were purchased as noted: poly A–poly U, poly (dAdT)₂, poly (dGdC)₂ and calf thymus ctDNA (Sigma-Aldrich). Polynucleotides were dissolved in Na-cacodylate buffer, $I = 0.05 \text{ mol dm}^{-3}$, pH = 7. The calf thymus ctDNA was additionally sonicated and filtered through a 0.45 μm filter [78]. Polynucleotide concentration was determined spectroscopically [79,80] as the concentration of phosphates. Spectrophotometric titrations were performed at pH = 7 ($I = 0.05 \text{ mol dm}^{-3}$, sodium cacodylate buffer) by adding portions of polynucleotide solution into the solution of the studied compound for fluorimetric experiments and for CD experiments were done by adding portions of compound stock solution into the solution of polynucleotide. In fluorimetric experiments excitation wavelength of $\lambda_{\text{exc}} = 317$ and 320 nm was used to avoid the inner filter effect caused due to increasing absorbance of the polynucleotide. Emission was collected in the range $\lambda_{\text{em}} = 330\text{--}700 \text{ nm}$. Values for K_s obtained by processing titration data by means of Scatchard equation [43], all have satisfactory correlation coefficients (>0.99). Thermal melting curves for DNA, RNA and their complexes with studied compounds were determined as previously described by following the absorption change at 260 nm as a function of temperature. Absorbance of the ligands was subtracted from every curve and the absorbance scale was normalized. T_m values are the midpoints of the transition curves determined from the maximum of the first derivative and checked graphically by the tangent method. The ΔT_m values were calculated subtracting T_m of the free nucleic acid from T_m of the complex. Every ΔT_m value here reported was the average of at least two measurements. The error in ΔT_m is $\pm 0.5^\circ\text{C}$.

4.5. Computational methods

Known inhibitors are retrieved from ChEMBL. Available X-ray structures of DNA complexes with small ligands were downloaded from the Protein data bank [51]. The ligand docking studies were carried out using Glide docking protocol with extra precision (XP) [81–84] within Schrödinger suite of software [85]. Binding poses were refined and binding energy was estimated using MM-GBSA [86–88] protocol and OPLS3 force-field with flexible residues distance being 5 Å. Molecular dynamic simulations were carried out using Desmond software within the Schrödinger package [89–91]. Simulations were carried out at the room temperature for 20 ns. *In silico* ADME properties as well as structural parameters were calculated by ACD/Percepta software [92].

4.6. *In vitro* ADME profiling

4.6.1. MDCKII-MDR1 permeability assay

MDCKII-hMDR1 cells were obtained from Solvo Biotechnology, Hungary. DMEM, Fetal bovine serum, Glutamax-100, Antibiotic/Antimycotic, DMSO, Dulbecco's phosphate buffer saline, MEM Non-essential amino acids were purchased from Sigma (St. Louis, MO, USA). Bi-directional permeability and P-glycoprotein substrate assessment were investigated in Madin-Darby canine epithelial cells with over-expressed human MDR1 gene (MDCKII-MDR1), coding for P-glycoprotein. Experimental procedures, as well as cell culture conditions, were the same as previously described [93]. Briefly, compounds (10 µM, 1% DMSO v/v) in duplicate were incubated at 37°C for 60 min with cell monolayer on 24-well Millicell inserts (Millipore, Burlington, MA, USA) without and with the P-glycoprotein inhibitor Elacridar (2 µM, International Laboratory, USA). Inhibition of P-glycoprotein was verified by amprenavir (Moravek Biochemicals Inc, Brea, CA, USA) and monolayer integrity by Lucifer yellow (Sigma, St. Louis, MO, USA). Compound concentrations were measured by LC-MS/MS and Lucifer yellow was measured on an Infinite F500 (Tecan, Männedorf, CH) using excitation of 485 nm and emission of 530 nm.

4.6.2. Metabolic stability

Mouse liver microsomes were obtained from Corning Life Sciences (Corning, USA). DMSO, nicotinamide adenine dinucleotide phosphate (NADP), glucose-6-phosphate, glucose-6-phosphate dehydrogenase, magnesium chloride, propranolol, caffeine, diclofenac, phosphate buffer saline (PBS) were purchased from Sigma (St. Louis, MO, USA). Acetonitrile (ACN) and methanol (MeOH) were obtained from Merck (Darmstadt, Germany). Testosterone was

purchased from Steraloids (Newport, RI, USA). Metabolic stability was assessed in mouse liver microsomes. Compounds (final concentration of 1 μ M, 0.03% DMSO v/v) were incubated in duplicate in phosphate buffer (50 mM, pH 7.4) at 37°C together with mouse liver microsomes in the absence and presence of the NADPH cofactor (0.5 mM nicotinamide adenine dinucleotide phosphate, 5 mM glucose-6-phosphate, 1.5 U/mL glucose-6-phosphate dehydrogenase and 0.5 mM magnesium chloride). Incubation and sampling was performed on a Freedom EVO 200 (Tecan, Männedorf, CH) at 0.3, 10, 20, 30, 45 and 60 min. The reaction was quenched using 3 volumes of a mixture of ACN/MeOH (2:1) containing internal standard (diclofenac), centrifuged and supernatants were analyzed using LC-MS/MS.

Metabolic activity of microsomes was verified by simultaneous analysis of several controls including testosterone, propranolol and caffeine. The in vitro half-life ($t_{1/2}$) was calculated using GraphPad Prism non-linear regression of % parent compound remaining versus time. In vitro clearance, expressed as μ L/min/mg, was estimated from the in vitro half-life ($t_{1/2}$), and normalized for the protein amount in the incubation mixture and assuming 52.5 mg of protein per gram of liver.

4.6.3. LC-MS/MS analysis

All samples were quantified using tandem mass spectrometry coupled to liquid chromatography. Samples were analysed on a Sciex API4000 Triple Quadrupole Mass Spectrometer (Sciex, Division of MDS Inc., Toronto, Canada) coupled to a Shimadzu Nexera X2 UHPLC frontend (Kyto, Japan). Samples were injected onto a UHPLC column (HALO2 C18, 2.1x20 mm, 2 μ m or Luna Omega 1.6 μ m Polar C18 100A, 30x2.1 mm) and eluted with a gradient at 50 °C. The mobile phase was composed of acetonitrile/water mixture (9/1, with 0.1 % formic acid) and 0.1 % formic acid in deionized water. The flow rate was 0.7 mL/min and under gradient conditions, leading to a total run time of 1.5–2 min. Positive ion mode with turbo spray, an ion source temperature of 550 °C and a dwell time of 150 ms were utilized for mass spectrometric detection. Quantitation was performed using multiple reaction monitoring (MRM) at the specific transitions for each compound.

Declaration of interest

Declaration of interest: none.

Acknowledgment

We greatly appreciate the financial support of the Croatian Science Foundation (project No. IP-2018-01-4682).

5. References

- [1] H.P. de Koning, The drugs of sleeping sickness: Their mechanisms of action and resistance, and a brief history, *Trop. Med. Infect. Dis.* 5 (2020) 14-37. <https://doi.org/10.3390/tropicalmed5010014>.
- [2] T. Von Geldern, M.O. Harhay, I. Scandale, R. Don, Kinetoplastid parasites, *Top. Med. Chem.* 7 (2011) 181-242. https://doi.org/10.1007/7355_2011_17.
- [3] W.M. Pardridge, The blood-brain barrier: Bottleneck in brain drug development, *NeuroRx.* 2 (2005) 3-14. <https://doi.org/10.1602/neurorx.2.1.3>.
- [4] Buckner, Buchynskyy, Nagendar, Patrick, Gillespie, Herbst, Tidwell, Gelb, Phenotypic Drug Discovery for Human African Trypanosomiasis: A Powerful Approach, *Trop. Med. Infect. Dis.* 5 (2020) E23. <https://doi.org/10.3390/tropicalmed5010023>.
- [5] J.C. Munday, L. Settimo, H.P. de Koning, Transport proteins determine drug sensitivity and resistance in a protozoan parasite, *Trypanosoma brucei*, *Front. Pharmacol.* 6 (2015) 32-42. <https://doi.org/10.3389/fphar.2015.00032>.
- [6] C.P. Ward, P.E. Wong, R.J. Burchmore, H.P. De Koning, M.P. Barrett, Trypanocidal furamide analogues: Influence of pyridine nitrogens on trypanocidal activity, transport kinetics, and resistance patterns, *Antimicrob. Agents Chemother.* 55 (2011) 2352-2361. <https://doi.org/10.1128/AAC.01551-10>.
- [7] M.N.C. Soeiro, E.M. De Souza, C.E. Stephens, D.W. Boykin, Aromatic diamidines as antiparasitic agents, *Expert Opin. Investig. Drugs.* 14 (2005) 957-972. <https://doi.org/10.1517/13543784.14.8.957>.
- [8] M.N.C. Soeiro, K. Werbovets, D.W. Boykin, W.D. Wilson, M.Z. Wang, A. Hemphill, Novel amidines and analogues as promising agents against intracellular parasites: A systematic review, *Parasitology.* 140 (2013) 929-951. <https://doi.org/10.1017/S0031182013000292>.

- [9] C.H. Ríos Martínez, J.J. Nué Martínez, G.U. Ebiloma, H.P. De Koning, I. Alkorta, C. Dardonville, Lowering the pKa of a bisimidazoline lead with halogen atoms results in improved activity and selectivity against *Trypanosoma brucei* in vitro, *Eur. J. Med. Chem.* 101 (2015) 806-817. <https://doi.org/10.1016/j.ejmech.2015.07.013>.
- [10] R.T. Jacobs, B. Nare, S.A. Wring, M.D. Orr, D. Chen, J.M. Sligar, M.X. Jenks, R.A. Noe, T.S. Bowling, L.T. Mercer, C. Rewerts, E. Gaukel, J. Owens, R. Parham, R. Randolph, B. Beaudet, C.J. Bacchi, N. Yarlett, J.J. Plattner, Y. Freund, C. Ding, T. Akama, Y.K. Zhang, R. Brun, M. Kaiser, I. Scandale, R. Don, Scyx-7158, an orally-active benzoxaborole for the treatment of stage 2 human african trypanosomiasis, *PLoS Negl. Trop. Dis.* 5 (2011) e1151. <https://doi.org/10.1371/journal.pntd.0001151>.
- [11] G. Eperon, M. Balasegaram, J. Potet, C. Mowbray, O. Valverde, F. Chappuis, Treatment options for second-stage gambiense human African trypanosomiasis, *Expert Rev. Anti. Infect. Ther.* 12 (2014) 1407-1417. <https://doi.org/10.1586/14787210.2014.959496>.
- [12] S.K. Andreassend, S.J. Bentley, G.L. Blatch, A. Boshoff, R.A. Keyzers, Screening for Small Molecule Modulators of *Trypanosoma brucei* Hsp70 Chaperone Activity Based upon Alcyonarian Coral-Derived Natural Products, *Mar. Drugs.* 18 (2020) e81. <https://doi.org/10.3390/md18020081>.
- [13] B.J. Fennell, J.A. Naughton, J. Barlow, G. Brennan, I. Fairweather, E. Hoey, N. McFerran, A. Trudgett, A. Bell, Microtubules as antiparasitic drug targets, *Expert Opin. Drug Discov.* 3 (2008) 501-518. <https://doi.org/10.1517/17460441.3.5.501>.
- [14] R. Docampo, S. Moreno, The Acidocalcisome as a Target for Chemotherapeutic Agents in Protozoan Parasites, *Curr. Pharm. Des.* 14 (2008) 882-888. <https://doi.org/10.2174/138161208784041079>.
- [15] S. Khare, A.S. Nagle, A. Biggart, Y.H. Lai, F. Liang, L.C. Davis, S.W. Barnes, C.J.N. Mathison, E. Myburgh, M.Y. Gao, J.R. Gillespie, X. Liu, J.L. Tan, M. Stinson, I.C. Rivera, J. Ballard, V. Yeh, T. Groessl, G. Federe, H.X.Y. Koh, J.D. Venable, B. Bursulaya, M. Shapiro, P.K. Mishra, G. Spraggon, A. Brock, J.C. Mottram, F.S. Buckner, S.P.S. Rao, B.G. Wen, J.R. Walker, T. Tuntland, V. Molteni, R.J. Glynne, F. Supek, Proteasome inhibition for treatment of leishmaniasis, Chagas disease and

- sleeping sickness, *Nature*. 537 (2016) 229-233. <https://doi.org/10.1038/nature19339>.
- [16] F.N. Penas, D. Carta, Á.C. Cevey, M.J. Rada, A.V. Pieralisi, M.G. Ferlin, M.E. Sales, G.A. Mirkin, N.B. Goren, Pyridinecarboxylic Acid Derivative Stimulates Pro-Angiogenic Mediators by PI3K/AKT/mTOR and Inhibits Reactive Nitrogen and Oxygen Species and NF- κ B Activation Through a PPAR γ -Dependent Pathway in *T. cruzi*-Infected Macrophages, *Front. Immunol.* 10 (2020) 2955-2970. <https://doi.org/10.3389/fimmu.2019.02955>.
- [17] M. Munde, M. Lee, S. Neidle, R. Arafa, D.W. Boykin, Y. Liu, C. Bailly, W.D. Wilson, Induced fit conformational changes of a “reversed amidine” heterocycle: Optimized interactions in a DNA minor groove complex, *J. Am. Chem. Soc.* 129 (2007) 5688-5698. <https://doi.org/10.1021/ja069003n>.
- [18] C.R. Millan, F.J. Acosta-Reyes, L. Lagartera, G.U. Ebiloma, L. Lemgruber, J.J.N. Martínez, N. Saperas, C. Dardonville, H.P. De Koning, J.L. Campos, Functional and structural analysis of AT-specific minor groove binders that disrupt DNA-protein interactions and cause disintegration of the *Trypanosoma brucei* kinetoplast, *Nucleic Acids Res.* 45 (2017) 8378-8391. <https://doi.org/10.1093/nar/gkx521>.
- [19] R. R. Tidwell, D. W. Boykin, Dicationic DNA minor groove binders as antimicrobial agents, in: M. Demeunynck, C. Bailly and W. D. Wilson (Eds.), *Small Molecule DNA and RNA Binders: From Synthesis to Nucleic Acid Complexes*, Wiley-VCH Verlag GmbH & Co. KGaA, Weinheim, 2002: pp: 414-460. <https://doi.org/10.1002/3527601783>.
- [20] A.B. Popov, I. Stolić, L. Krstulović, M.C. Taylor, J.M. Kelly, S. Tomić, L. Tumir, M. Bajić, S. Raić-Malić, Novel symmetric bis-benzimidazoles: Synthesis, DNA/RNA binding and antitrypanosomal activity, *Eur. J. Med. Chem.* 173 (2019) 63-75. <https://doi.org/10.1016/j.ejmech.2019.04.007>.
- [21] A. Bistrović, L. Krstulović, I. Stolić, D. Drenjančević, J. Talapko, M.C. Taylor, J.M. Kelly, M. Bajić, S. Raić-Malić, Synthesis, anti-bacterial and anti-protozoal activities of amidinobenzimidazole derivatives and their interactions with DNA and RNA, *J. Enzyme Inhib. Med. Chem.* 33 (2018) 271-285. <https://doi.org/10.1080/14756366.2018.1484733>.

- [22] R.M.B.M. Girard, M. Crispim, I. Stolić, F.S. Damasceno, M.S. Da Silva, E.M.F. Pral, M.C. Elias, M. Bajić, A.M. Silber, An aromatic diamidine that targets kinetoplast DNA, impairs the cell cycle in *Trypanosoma cruzi*, and diminishes trypomastigote release from infected mammalian host cells, *Antimicrob. Agents Chemother.* 60 (2016) 5867-5877. <https://doi.org/10.1128/AAC.01595-15>.
- [23] G.E. Miana, S.R. Ribone, D.M.A. Vera, M. Sánchez-Moreno, M.R. Mazzieri, M.A. Quevedo, Design, synthesis and molecular docking studies of novel N-arylsulfonyl-benzimidazoles with anti *Trypanosoma cruzi* activity, *Eur. J. Med. Chem.* 165 (2019) 1-10. <https://doi.org/10.1016/j.ejmech.2019.01.013>.
- [24] A.A. Farahat, M.A. Ismail, A. Kumar, T. Wenzler, R. Brun, A. Paul, W.D. Wilson, D.W. Boykin, Indole and Benzimidazole Bichalcophenes: Synthesis, DNA Binding and Antiparasitic Activity, *Eur. J. Med. Chem.* 143 (2018) 1590-1596. <https://doi.org/10.1016/j.ejmech.2017.10.056>.
- [25] S. Melchor-Doncel de la Torre, C. Vázquez, Z. González-Chávez, L. Yépez-Mulia, R. Nieto-Meneses, R. Jasso-Chávez, E. Saavedra, F. Hernández-Luis, Synthesis and biological evaluation of 2-methyl-1H-benzimidazole-5-carbohydrazides derivatives as modifiers of redox homeostasis of *Trypanosoma cruzi*, *Bioorganic Med. Chem. Lett.* 27 (2017) 3403-3407. <https://doi.org/10.1016/j.bmcl.2017.06.013>.
- [26] S. Oh, S. Kim, S. Kong, G. Yang, N. Lee, D. Han, J. Goo, J.L. Siqueira-Neto, L.H. Freitas-Junior, R. Song, Synthesis and biological evaluation of 2,3-dihydroimidazo[1,2-a] benzimidazole derivatives against *Leishmania donovani* and *Trypanosoma cruzi*, *Eur. J. Med. Chem.* 84 (2014) 395-403. <https://doi.org/10.1016/j.ejmech.2014.07.038>.
- [27] M. Alp, H. Göker, R. Brun, S. Yildiz, Synthesis and antiparasitic and antifungal evaluation of 2'-arylsubstituted-1H,1'H-[2,5']bisbenzimidazolyl-5-carboxamidines, *Eur. J. Med. Chem.* 44 (2009) 2002-2008. <https://doi.org/10.1016/j.ejmech.2008.10.003>.
- [28] J.M. Velázquez-López, A. Hernández-Campos, L. Yépez-Mulia, A. Téllez-Valencia, P. Flores-Carrillo, R. Nieto-Meneses, R. Castillo, Synthesis and trypanocidal activity of novel benzimidazole derivatives, *Bioorganic Med. Chem. Lett.* 26 (2016) 4377-4381.

<https://doi.org/10.1016/j.bmcl.2015.08.018>.

- [29] M. Boiani, L. Boiani, A. Merlino, P. Hernández, A. Chidichimo, J.J. Cazzulo, H. Cerecetto, M. González, Second generation of 2H-benzimidazole 1,3-dioxide derivatives as anti-trypanosomatid agents: Synthesis, biological evaluation, and mode of action studies, *Eur. J. Med. Chem.* 44 (2009) 4426-4433.
<https://doi.org/10.1016/j.ejmech.2009.06.014>.
- [30] C. Karaaslan, M. Kaiser, R. Brun, H. Göker, Synthesis and potent antiprotozoal activity of mono/di amidino 2-anilinobenzimidazoles versus *Plasmodium falciparum* and *Trypanosoma brucei rhodesiense*, *Bioorganic Med. Chem.* 24 (2016) 4038-4044.
<https://doi.org/10.1016/j.bmc.2016.06.047>.
- [31] E.D. Deeks, Fexinidazole: First Global Approval, *Drugs.* 79 (2019) 215-220.
<https://doi.org/10.1007/s40265-019-1051-6>.
- [32] E. Torreele, B.B. Trunz, D. Tweats, M. Kaiser, R. Brun, G. Mazué, M.A. Bray, B. Pécoul, Fexinidazole - a new oral nitroimidazole drug candidate entering clinical development for the treatment of sleeping sickness, *PLoS Negl. Trop. Dis.* 4 (2010) e923. <https://doi.org/10.1371/journal.pntd.0000923>.
- [33] H. Burrell-Saward, A.J. Harris, R. de LaFlor, H. Sallam, M.S. Alavijeh, T.H. Ward, S.L. Croft, Dose-dependent effect and pharmacokinetics of fexinidazole and its metabolites in a mouse model of human African trypanosomiasis, *Int. J. Antimicrob. Agents.* 50 (2017) 203-209. <https://doi.org/10.1016/j.ijantimicag.2017.01.038>.
- [34] V. Lutje, J. Seixas, A. Kennedy, Chemotherapy for second-stage Human African trypanosomiasis, *Cochrane Database Syst. Rev.* 6 (2013) CD006201.
<https://doi.org/10.1002/14651858.CD006201.pub3>.
- [35] S.A. Bakunov, S.M. Bakunova, T. Wenzler, M. Ghebru, K.A. Werbovets, R. Brun, R.R. Tidwell, Synthesis and antiprotozoal activity of cationic 1,4-diphenyl-1H-1,2,3-triazoles, *J. Med. Chem.* 53 (2010) 254-272. <https://doi.org/10.1021/jm901178d>.
- [36] P. Nagendar, J.R. Gillespie, Z.M. Herbst, R.M. Ranade, N.M.R. Molasky, O. Faghieh, R.M. Turner, M.H. Gelb, F.S. Buckner, Triazolopyrimidines and Imidazopyridines: Structure-Activity Relationships and in Vivo Efficacy for Trypanosomiasis, *ACS Med.*

- Chem. Lett. 10 (2019) 105-110. <https://doi.org/10.1021/acsmchemlett.8b00498>.
- [37] M. Hranjec, K. Starčević, B. Zamola, S. Mutak, M. Derek, G. Karminski-Zamola, New amidino-benzimidazolyl derivatives of tylosin and desmycosin, *J. Antibiot. (Tokyo)* 55 (2002) 308-314. <https://doi.org/10.7164/antibiotics.55.308>.
- [38] D. Havrylyuk, B. Zimenkovsky, O. Karpenko, P. Grellier, R. Lesyk, Synthesis of pyrazoline-thiazolidinone hybrids with trypanocidal activity, *Eur. J. Med. Chem.* 85 (2014) 245-254. <https://doi.org/10.1016/j.ejmech.2014.07.103>.
- [39] P. O'Sullivan, I. Rozas, Understanding the guanidine-like cationic moiety for optimal binding into the DNA minor groove, *ChemMedChem.* 9 (2014) 2065-2073. <https://doi.org/10.1002/cmdc.201402264>.
- [40] C.H. Ríos Martínez, L. Lagartera, C. Trujillo, C. Dardonville, Bisimidazoline arylamides binding to the DNA minor groove: N1-hydroxylation enhances binding affinity and selectivity to AATT sites, *MedChemComm.* 6 (2015) 2036-2042. <https://doi.org/10.1039/c5md00292c>.
- [41] W. Saenger, Synthetic, Homopolymer Nucleic Acids Structures, in: W. Saenger (Ed), *Principles of nucleic acid structure*, 1st ed., Springer-Verlag New York, 1984: pp. 298-320. <https://doi.org/10.1007/978-1-4612-5190-3>.
- [42] C.R. Cantor, P.R. Schimmel, The behaviour of biological macromolecules, in: C.R. Cantor, P.R. Schimmel (Eds), *Biophysical Chemistry*, 1st ed., W.H. Freeman & Co., San Francisco, 1980: pp. 1109-1114.
- [43] G. Scatchard, The attractions of proteins for small molecules and ions, *Ann. N. Y. Acad. Sci.* 51 (1949) 660-672. <https://doi.org/10.1111/j.1749-6632.1949.tb27297.x>.
- [44] J.L. Mergny, L. Lacroix, Analysis of Thermal Melting Curves, *Oligonucleotides.* 13 (2003) 515-537. <https://doi.org/10.1089/154545703322860825>.
- [45] M. Radić Stojković, S. Miljanić, K. Mišković, L. Glavaš-Obrovac, I. Piantanida, The phenanthridine biguanides efficiently differentiate between dGdC, dAdT and rArU sequences by two independent, sensitive spectroscopic methods, *Mol. Biosyst.* 7 (2011) 1753-1765. <https://doi.org/10.1039/c1mb05030c>.
- [46] A. Rodger, Circular Dichroism and Linear Dichroism, in: *Encyclopedia of Analytical*

Chemistry: Applications, Theory and Instrumentation, Online © 2006–2013 John Wiley & Sons, Ltd., 2014: pp. 1–34.

<https://doi.org/10.1002/9780470027318.a5402.pub2>.

- [47] N. Berova, K. Nakanishi (Eds), *Circular Dichroism: Principles and Applications*, 2nd ed., Wiley-VCH, New York, 2000.
- [48] M. Eriksson, B. Nordén, Linear and circular dichroism of drug-nucleic acid complexes, in: J. B. Chaires, M. J. Waring (Eds), *Methods in Enzymology*. Vol. 340. *Drug–Nucleic Acid Interactions*, 1st ed., Academic Press, New York. 2001: pp. 68-98.
- [49] T. Šmidlehner, I. Piantanida, G. Pescitelli, Polarization spectroscopy methods in the determination of interactions of small molecules with nucleic acids - Tutorial, *Beilstein J. Org. Chem.* 14 (2017) 84-105. <https://doi.org/10.3762/bjoc.14.5>.
- [50] M. Radić Stojković, I. Piantanida, Tuning urea-phenanthridinium conjugates for DNA/RNA and base pair recognition, *Tetrahedron*. 64 (2008) 7807-7814. <https://doi.org/10.1016/j.tet.2008.05.142>.
- [51] H.M. Berman, J. Westbrook, Z. Feng, G. Gilliland, T.N. Bhat, H. Weissig, I.N. Shindyalov, The Protein Data Bank (www.rcsb.org), *Nucleic Acids Res.* 28 (2000) 235-242. <https://doi.org/10.1093/nar/28.1.235>.
- [52] S.K. Burley, H.M. Berman, C. Bhikadiya, C. Bi, L. Chen, L. Di Costanzo, C. Christie, K. Dalenberg, J.M. Duarte, S. Dutta, Z. Feng, S. Ghosh, D.S. Goodsell, R.K. Green, V. Guranović, D. Guzenko, B.P. Hudson, T. Kalro, Y. Liang, R. Lowe, H. Namkoong, E. Peisach, I. Periskova, A. Prlić, C. Randle, A. Rose, P. Rose, R. Sala, M. Sekharan, C. Shao, L. Tan, Y.P. Tao, Y. Valasatava, M. Voigt, J. Westbrook, J. Woo, H. Yang, J. Young, M. Zhuravleva, C. Zardecki, RCSB Protein Data Bank: Biological macromolecular structures enabling research and education in fundamental biology, biomedicine, biotechnology and energy, *Nucleic Acids Res.* 47 (2019) D464-D474. <https://doi.org/10.1093/nar/gky1004>.
- [53] M.L. Barcellona, E. Gratton, Fluorescence lifetime distributions of DNA-4',6-diamidino-2-phenylindole complex, *BBA - Gen. Subj.* 993 (1989) 174-178. [https://doi.org/10.1016/0304-4165\(89\)90160-8](https://doi.org/10.1016/0304-4165(89)90160-8).

- [54] B. Nguyen, M.P.H. Lee, D. Hamelberg, A. Joubert, C. Bailly, R. Brun, S. Neidle, W.D. Wilson, Strong binding in the DNA minor groove by an aromatic diamidine with a shape that does not match the curvature of the groove, *J. Am. Chem. Soc.* 124 (2002) 13680-13681. <https://doi.org/10.1021/ja027953c>.
- [55] Y. Miao, M.P.H. Lee, G.N. Parkinson, A. Batista-Parra, M.A. Ismail, S. Neidle, D.W. Boykin, W.D. Wilson, Out-of-shape DNA minor groove binders: Induced fit interactions of heterocyclic dication with the DNA minor groove, *Biochemistry*. 44 (2005) 14701-14708. <https://doi.org/10.1021/bi051791q>.
- [56] S. Mukherjee, S. Kundu, D. Bhattacharyya, Temperature effect on poly(dA).poly(dT): Molecular dynamics simulation studies of polymeric and oligomeric constructs, *J. Comput. Aided. Mol. Des.* 28 (2014) 735-749. <https://doi.org/10.1007/s10822-014-9755-x>.
- [57] M. Lůkov, S. Tshepelevitsh, A. Heering, P.G. Plieger, R. Vianello, I. Leito, On the Basicity of Conjugated Nitrogen Heterocycles in Different Media, *European J. Org. Chem.* 2019 (2017) 4475-4489. <https://doi.org/10.1002/ejoc.201700749>.
- [58] E.D. Raczynska, General structure–basicity relations for trisubstituted acetamidines, *J. Chem. Soc. Perkin Trans. 2.* (1987) 1117-1110. <https://doi.org/10.1039/P29870001117>.
- [59] H.K. Hall, R.B. Bates, Correlation of alkylamine nucleophilicities with their basicities, *Tetrahedron Lett.* 53 (2012) 1830-1832. <https://doi.org/10.1016/j.tetlet.2012.01.128>.
- [60] C. Fleau, A. Padilla, J. Miguel-Siles, M.T. Quesada-Campos, I. Saiz-Nicolas, I. Cotillo, J. Cantizani Perez, R.L. Tarleton, M. Marco, G. Courtemanche, Chagas Disease Drug Discovery: Multiparametric Lead Optimization against *Trypanosoma cruzi* in Acylaminobenzothiazole Series, *J. Med. Chem.* 62 (2019) 10362-10375. <https://doi.org/10.1021/acs.jmedchem.9b01429>.
- [61] N.T. Chandrika, S.K. Shrestha, H.X. Ngo, S. Garneau-Tsodikova, Synthesis and investigation of novel benzimidazole derivatives as antifungal agents, *Bioorg. Med. Chem.* 24 (2016) 3680-3686. <https://doi.org/10.1016/j.bmc.2016.06.010>.
- [62] P.A. Greenidge, C. Kramer, J.C. Mozziconacci, R.M. Wolf, MM/GBSA binding energy prediction on the PDBbind data set: Successes, failures, and directions for

- further improvement, *J. Chem. Inf. Model.* 53 (2013) 201-209.
<https://doi.org/10.1021/ci300425v>.
- [63] C. Xiao, Y. Cheng, Y. Zhang, J. Ding, C. He, X. Zhuang, X. Chen, Side chain impacts on pH- and thermo-responsiveness of tertiary amine functionalized polypeptides, *J. Polym. Sci. Part A Polym. Chem.* 52 (2014) 671-679.
<https://doi.org/10.1002/pola.27048>.
- [64] R. Kumar, J. Arora, A.K. Prasad, N. Islam, A.K. Verma, Synthesis and antimicrobial activity of pyrimidine chalcones, *Med. Chem. Res.* 22 (2013) 56624-5631.
<https://doi.org/10.1007/s00044-013-0555-y>.
- [65] T.S. Rodrigues, A.G.M. da Silva, L.C. de Oliveira, A.M. da Silva, R.R. Teixeira, P.H.C. Camargo, Cu₂O spheres as an efficient source of catalytic Cu(I) species for performing azide-alkyne click reactions, *Tetrahedron Lett.* 58 (2017) 590-595.
<https://doi.org/10.1016/j.tetlet.2017.01.005>.
- [66] T.T.T. Maulik R. Patel, Aaditya Bhatt, Jamin D. Steffen, Adel Chergui, Junko Murai, Yves Pommier, John M. Pascal, Louis D. Trombetta, Frank R. Fronczek, Discovery and structure-activity relationship of novel 2,3-dihydrobenzofuran-7-carboxamide and 2,3-dihydrobenzofuran-3(2H)-one-7-carboxamide derivatives as poly(ADP-ribose)polymerase-1 inhibitors, *J. Med. Chem.* 57 (2014) 5579-5601.
<https://doi.org/10.1021/jm5002502>.
- [67] K.R. Senwar, T.S. Reddy, D. Thummuri, P. Sharma, V.G.M. Naidu, G. Srinivasulu, N. Shankaraiah, Design, synthesis and apoptosis inducing effect of novel (Z)-3-(3'-methoxy-4'-(2-amino-2-oxoethoxy)-benzylidene)indolin-2-ones as potential antitumour agents, *Eur. J. Med. Chem.* 118 (2016) 34-46.
<https://doi.org/10.1016/j.ejmech.2016.04.025>.
- [68] T.Y. Zhang, Z.K. Yu, X.J. Jin, M.Y. Li, L.P. Sun, C.J. Zheng, H.R. Piao, Synthesis and evaluation of the antibacterial activities of aryl substituted dihydrotriazine derivatives, *Bioorg. Med. Chem. Lett.* 28 (2018) 1657-1662.
<https://doi.org/10.1016/j.bmcl.2018.03.037>.
- [69] X. Bu, H. Jing, L. Wang, T. Chang, L. Jin, Y. Liang, Organic base catalyzed O-alkylation of phenols under solvent-free condition, *J. Mol. Catal. A Chem.* 259 (2006)

121-124. <https://doi.org/10.1016/j.molcata.2006.06.009>.

- [70] N.W. Keigo Tanaka, Eiichi Yamamoto, Pyridine derivative substituted with heterocycle and phosphonoamino and antifungal agent containing the same, WO2008136324A1, 2008.
- [71] I.N. Nnamani, G.S. Joshi, R. Danso-Danquah, O. Abdulmatik, T. Asakuru, D.J. Abraham, M.K. Safo, Pyridyl derivatives of benzaldehyde as potential antisickling agents, *Chem. Biodivers.* 5 (2008) 1762-1769.
<https://doi.org/10.1002/cbdv.200890165>.
- [72] Y. Pourshojaei, A. Gouranourimi, S. Hekmat, A. Asadipour, S. Rahmani-Nezhad, A. Moradi, H. Nadri, F.H. Moghadam, S. Emami, A. Foroumadi, A. Shafiee, Design, synthesis and anticholinesterase activity of novel benzylidenechroman-4-ones bearing cyclic amine side chain, *Eur. J. Med. Chem.* 97 (2015) 181-189.
<https://doi.org/10.1016/j.ejmech.2015.04.055>.
- [73] A.S. Judd, A.J. Souers, D. Wodka, G. Zhao, M.M. Mulhern, R.R. Iyengar, J. Gao, J.K. Lynch, J.C. Freeman, H.D. Falls, S. Brodjian, B.D. Dayton, R.M. Reilly, G. Gintant, J.T. Limberis, A. Mikhail, S.T. Leitza, K.A. Houseman, G. Diaz, E.N. Bush, R. Shapiro, V. Knourek-Segel, L.E. Hernandez, K.C. Marsh, H.L. Sham, C.A. Collins, P.R. Kym, Identification of diamino chromone-2-carboxamides as MCHR1 antagonists with minimal hERG channel activity, *Bioorg. Med. Chem. Lett.* 17 (2007) 2365-2371.
<https://doi.org/10.1016/j.bmcl.2006.11.068>.
- [74] R. Bansal, G. Kumar, S. Rohilla, K.N. Klotz, S. Kachler, L.C. Young, A.L. Harvey, Synthesis and Evaluation of a New Series of 8-(2-Nitroaryl)Xanthines as Adenosine Receptor Ligands, *Drug Dev. Res.* 77 (2016) 241-250.
<https://doi.org/10.1002/ddr.21317>.
- [75] Y. Yadav, E.D. MacLean, A. Bhattacharyya, V.S. Parmar, J. Balzarini, C.J. Barden, C.K.L. Too, A. Jha, Design, synthesis and bioevaluation of novel candidate selective estrogen receptor modulators, *Eur. J. Med. Chem.* 46 (2011) 3858-3866.
<https://doi.org/10.1016/j.ejmech.2011.05.054>.
- [76] R. Bansal, G. Kumar, D. Gandhi, L.C. Young, A.L. Harvey, Synthesis of a series of 8-(substituted-phenyl)xanthines and a study on the effects of substitution pattern of

- phenyl substituents on affinity for adenosine A1 and A2A receptors, *Eur. J. Med. Chem.* 44 (2009) 2122-2127. <https://doi.org/10.1016/j.ejmech.2008.10.017>.
- [77] M.C. Taylor, M.D. Lewis, A.F. Francisco, S.R. Wilkinson, J.M. Kelly, The Trypanosoma cruzi Vitamin C Dependent Peroxidase Confers Protection against Oxidative Stress but Is Not a Determinant of Virulence, *PLoS Negl. Trop. Dis.* 9 (2015) e000370. <https://doi.org/10.1371/journal.pntd.0003707>.
- [78] J.B. Chaires, N. Dattagupta, D.M. Crothers, Studies on Interaction of Anthracycline Antibiotics and Deoxyribonucleic Acid: Equilibrium Binding Studies on Interaction of Daunomycin with Deoxyribonucleic Acid, *Biochemistry.* 21 (1982) 3933-3940. <https://doi.org/10.1021/bi00260a005>.
- [79] J.L. Bresloff, D.M. Crothers, Equilibrium Studies of Ethidium-Polynucleotide Interactions, *Biochemistry.* 20 (1981) 3547-3553. <https://doi.org/10.1021/bi00515a038>.
- [80] T. V. Chalikian, J. Völker, G.E. Plum, K.J. Breslauer, A more unified picture for the thermodynamics of nucleic acid duplex melting: A characterization by calorimetric and volumetric techniques, *Proc. Natl. Acad. Sci. USA.* 96 (1999) 7853-7858. <https://doi.org/10.1073/pnas.96.14.7853>.
- [81] R.A. Friesner, R.B. Murphy, M.P. Repasky, L.L. Frye, J.R. Greenwood, T.A. Halgren, P.C. Sanschagrín, D.T. Mainz, Extra precision glide: Docking and scoring incorporating a model of hydrophobic enclosure for protein-ligand complexes, *J. Med. Chem.* 49 (2006) 6177-6196. <https://doi.org/10.1021/jm051256o>.
- [82] T.A. Halgren, R.B. Murphy, R.A. Friesner, H.S. Beard, L.L. Frye, W.T. Pollard, J.L. Banks, Glide: A New Approach for Rapid, Accurate Docking and Scoring. 2. Enrichment Factors in Database Screening, *J. Med. Chem.* 47 (2004) 1750-1759. <https://doi.org/10.1021/jm030644s>.
- [83] R.A. Friesner, J.L. Banks, R.B. Murphy, T.A. Halgren, J.J. Klicic, D.T. Mainz, M.P. Repasky, E.H. Knoll, M. Shelley, J.K. Perry, D.E. Shaw, P. Francis, P.S. Shenkin, Glide: A New Approach for Rapid, Accurate Docking and Scoring. 1. Method and Assessment of Docking Accuracy, *J. Med. Chem.* 47 (2004) 1739-1749. <https://doi.org/10.1021/jm030643o>.

- [84] Schrödinger Release 2019-3: Glide, Schrödinger, LLC, New York, NY, (2019).
- [85] Schrödinger Release 2019-3, Schrödinger, LLC, New York, NY, (2017).
- [86] J. Li, R. Abel, K. Zhu, Y. Cao, S. Zhao, R.A. Friesner, The VSGB 2.0 model: A next generation energy model for high resolution protein structure modeling, *Proteins Struct. Funct. Bioinforma.* 79 (2011) 2794-2812. <https://doi.org/10.1002/prot.23106>.
- [87] W.L. Jorgensen, D.S. Maxwell, J. Tirado-Rives, Development and testing of the OPLS all-atom force field on conformational energetics and properties of organic liquids, *J. Am. Chem. Soc.* 118 (1996) 11225-11236. <https://doi.org/10.1021/ja9621760>.
- [88] D. Shivakumar, J. Williams, Y. Wu, W. Damm, J. Shelley, W. Sherman, Prediction of absolute solvation free energies using molecular dynamics free energy perturbation and the opls force field, *J. Chem. Theory Comput.* 6 (2010) 1509-1519. <https://doi.org/10.1021/ct900587b>.
- [89] K.J. Bowers, E. Chow, H. Xu, R.O. Dror, M.P. Eastwood, B.A. Gregersen, J.L. Klepeis, I. Kolossvary, M.A. Moraes, F.D. Sacerdoti, J.K. Salmon, Y. Shan, D.E. Shaw, Scalable algorithms for molecular dynamics simulations on commodity clusters, in: *Proc. 2006 ACM/IEEE Conf. Supercomput. SC'06, 2006*. <https://doi.org/10.1145/1188455.1188544>.
- [90] Schrödinger Release 2019-3: Desmond Molecular Dynamics System, D. E. Shaw Research, New York, NY, (2019).
- [91] Maestro-Desmond Interoperability Tools, Schrödinger, New York, NY, (2019).
- [92] ACD/Percepta, version 2017.2.1, Advanced Chemistry Development, Inc., Toronto, On, Canada, www.acdlabs.com, (2019).
- [93] P. Acharya, M.P. O'Connor, J.W. Polli, A. Ayrton, H. Ellens, J. Bentz, Kinetic Identification of Membrane Transporters That Assist P-glycoprotein-Mediated Transport of Digoxin and Loperamide through a Confluent Monolayer of MDCKII-hMDR1 Cells. *Drug Metab. Dispos.* 36 (2008) 452-460. <https://doi.org/10.1124/dmd.107.017301>.